THE JOURNAL OF CHEMICAL PHYSICS VOLUME 59, NUMBER 2 15 JULY 1973

Proton-enhanced NMR of dilute spins in solids*

A. Pines†, M. G. Gibby‡, and J. S. Waugh

Department of Chemistry and Research Laboratory of Electronics, Massachusetts Institute of Technology, Cambridge, Massachusetts 02139

(Received 14 February 1973)

The NMR signals of isotopically or chemically dilute nuclear spins S in solids can be enhanced by repeatedly transferring polarization from a more abundant species I of high abundance (usually protons) to which they are coupled. The gain in power sensitivity as compared with conventional observation of the rare spins approaches $N_I I(I+1)\gamma_I^2/N_S S(S+1)\gamma_S^2$, or $\approx 10^3$ for $S = {}^{13}C$, $I = {}^1H$ in organic solids. The transfer of polarization is accomplished by any of a number of double resonance methods. High-frequency resolution of the S-spin signal is obtained by decoupling of the abundant spins. The experimental requirements of the technique are discussed and a brief comparison of its sensitivity with other procedures is made. Representative applications and experimental results are mentioned.

I. INTRODUCTION

Although high-resolution NMR in liquids is established as a powerful tool for structural and dynamical studies of chemical systems,[1] analogous experiments on solids have enjoyed a more limited prosperity. The reason is well known: whereas the direct nuclear magnetic dipole–dipole interaction is averaged to zero in liquids due to rapid rotational and translational diffusion, no such motion prevails in rigid solids, leaving the above interaction as an annoying source of spectral broadening. If we consider that spectral structure due to chemical shifts and spin–spin couplings requires resolution of approximately several hertz, while dipolar broadening is normally of approximately several kilohertz, it is clear that we are faced with a real problem if we wish to bring solids into the realm of conventional high-resolution NMR.

In many instances, it is precisely the dipolar interaction in a solid which is at the center of attention (or its presence is a crucial factor). Such is the case, for example, in studies of line shapes,[2] spin diffusion,[3] spin temperature,[4] etc. In addition, it can be used to good advantage in both structural and dynamical studies, as exemplified by wide-line dipolar structure[5] and by second moment and spin–lattice relaxation studies of motion.[6] It is clear, however, that a considerable increase in information could be attained if it were possible to suppress the dipolar broadening and extract details on other interactions such as chemical shifts and indirect nuclear spin–spin couplings. The type of information from solids should be valuable, since the restriction of molecular reorientation preserves any anisotropy (e.g., chemical shielding anisotropy) which is averaged to zero in liquid systems and may show up only indirectly through spin relaxation effects.

Several approaches have been made to this important problem. They may be discussed in terms of the Hamiltonian for the "truncated" dipolar interactions[7] in a substance containing two species, I and S, of different magnetogyric ratios γ_I and γ_s:

$$\begin{aligned}
\mathcal{H}_d^0 &= \mathcal{H}_{II}^0 + \mathcal{H}_{SS}^0 + \mathcal{H}_{IS}^0 , \\
\mathcal{H}_{II}^0 &= \gamma_I^2 \hbar^2 \sum_{i<j}^{N_I}\sum r_{ij}^{-3} P_2(\cos\theta_{ij})(\mathbf{I}_i \cdot \mathbf{I}_j - 3I_{iz}I_{jz}) , \\
\mathcal{H}_{SS}^0 &= \gamma_S^2 \hbar^2 \sum_{m<n}^{N_S}\sum r_{mn}^{-3} P^2(\cos\theta_{mn})(\mathbf{S}_m \cdot \mathbf{S}_n - 3S_{mz}S_{nz}) , \qquad (1) \\
\mathcal{H}_{IS}^0 &= 2\gamma_I\gamma_S \hbar^2 \sum_{i=1}^{N_I} \sum_{m=1}^{N_S} r_{im}^{-3} P_2(\cos\theta_{im}) I_{iz}S_{mz} , \\
&= \sum_{m=1}^{N_S} S_{mz} \sum_{i=1}^{N_I} b_{im} I_{iz} .
\end{aligned}$$

The techniques and their effects differ according to the nature of the sample and to which part of (1) they choose to affect. In the magic-angle sample-spinning experiment,[8–10] the θ's are modulated rapidly giving $\langle P_2[\cos\theta(t)]\rangle = 0$, all i, j, m, n, so that all dipolar interactions are erased. At the same time, all other anisotropic interactions transforming as second-rank tensors, such as the anisotropic part of the chemical shift, are also removed. In multiple-pulse *NMR*,[11–14] in an appropriate reference frame, it is $\mathbf{I}$ that is modulated, giving $\langle 3I_{iz}(t)I_{jz}(t) - \mathbf{I}_i \cdot \mathbf{I}_j\rangle = 0$. Thus the dipolar interactions are fully removed only in a single-species sample ($N_S = 0$). The anisotropic chemical shift is, however, not lost. Both methods have met with considerable success. The sample-spinning requires high rotation speeds ($\gtrsim 10$ kHz) making it difficult for rigid solids. The multiple-pulse techniques, on the other hand, require high rf phase and amplitude stability, and despite the promise of enhanced resolution through the use of symmetry,[15–19] resonance-offset effects,[20,21] and computer-aided adjustments,[22] they are difficult to perform routinely.

In the present paper we discuss a different approach which we find to be rather simple and widely applicable, and which has produced a significant flux of preliminary experimental results since its recent institution.[23] The basic premise is remarkably simple: It depends upon having $N_I \gg N_S$ by virtue of high chemical or isotopic dilution of the S spins (e.g., ^{13}C) in a matrix of abundant I spins (e.g., ^1H). Under such circumstances $\mathcal{H}^0_{SS}$ becomes small and can often be neglected because of the large values typical of r_{mn}. (If in addition $N_I = 0$, of course all dipolar broadening is removed without further ado.) Precisely this thinking motivated the experiment of Lauterbur on $Ca^{13}CO_3$[24] and those of Pines, Rhim, and Waugh on $Ca^{13}CO_3$ and $^{13}CS_2$.[25] The ^{13}C and ^{15}N constitute ideal nuclei for such studies since they have both low magnetogyric ratios and low isotopic abundance.

However, *much* more commonly, rare spins such as ^{13}C and ^{15}N experience severe dipolar broadening by abundant spins, usually protons. In addition, whether or not this is the case, the obvious price which we must pay for the attenuation of dipolar interaction between the S spins is a reduction of the number of resonant spins in the sample and a consequent reduction in the sensitivity of NMR detection. This problem is a well-known one in liquid studies of rare isotopes, where Fourier-transform and signal averaging techniques must be employed to their full extent.[26,27] In solids, where resolution is lower and spin-lattice relaxation times may be very long, the problem of detection becomes much more acute, making conventional techniques essentially useless.

Lest the reader despair, we remark that both of the problems mentioned above—those of resolution and of sensitivity—can be solved with surprising facility. Dipolar broadening by unlike spins is removed by strong irradiation of these spins at their resonance frequency.[28,29] As in the case of J coupling in liquids, this induces a "spin decoupling."[30] The power requirements in the solid case are much greater due to the strength of the dipolar interaction relative to J coupling. It might appear that this spin decoupling should be as difficult as the removal of dipolar interactions between like spins making it similar to multiple-pulse experiments. However, it is actually much simpler due to the simpler transformation properties of the resonant spin operators, and the stability requirements on rf phase and amplitude are considerably less stringent.

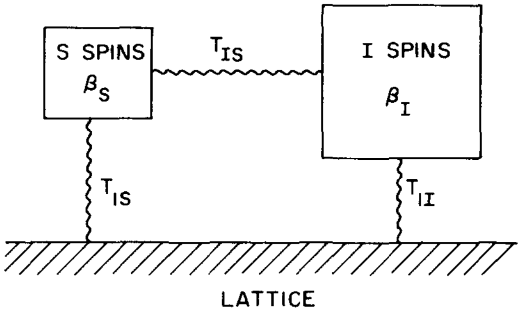

FIG. 1. Simple thermodynamic picture for double resonance. T_{1S} and T_{1I} are nuclear spin-lattice relaxation times which are imagined to be very long, and T_{IS} is a cross-relaxation time. The two energy reservoirs of I and S spins are at inverse spin temperatures β_I and β_S. In the classical indirect detection method, the I spins are cooled by allowing them to equilibrate for $\sim T_{1I}$ with the lattice. The S spins are detected by bringing them into contact with the I-spin reservoir and keeping them hot by one of several techniques. Energy flows at a rate of $\sim \epsilon/T_{IS}$ from the S- to the I-spin reservoir (where ϵ is the ratio of S to I heat capacities) causing a cumulative heating and destruction of the I-spin order. Subsequent observation of a reduced I signal indicates the S resonance. The sensitivity demands that I spin order be maintained for long times $\sim T_{IS}/\epsilon$. In the direct detection method, the I-spin reservoir is used only as a source of polarization and is not observed. Following an I–S contact (the S spins are not kept hot here), the S spins are observed directly, and the signals co-added $\sim 1/\epsilon$ times to yield a markedly enhanced S spectrum within one T_{1I}.

The sensitivity problem is similarly approached by adapting an idea established by Hartmann and Hahn.[31] In the Hartmann–Hahn experiment, a system of rare spins (S) is detected by observing its accumulative effects on an abundant spin system. The language of spin thermodynamics[4,32] is well suited to a discussion of these phenomena (see Fig. 1). Basically, the experiment works as follows: the I spin system is brought into equilibrium with the lattice at an inverse temperature $\beta_L = (kT_L)^{-1}$. Normally, a large magnetization $\gamma\hbar\langle I\rangle \propto N_I\beta_L$ could now be observed. Instead, the I spins are now brought into contact with the S spins which are imagined to have no spin order, i.e., an infinite spin temperature. The contact can be established in many ways, some of which will be discussed later in this paper. The simplest to visualize is the application of two strong rf fields, H_{1I} and H_{1S}, at the I and S resonance frequencies. The former is arranged by one of several methods to spin lock[20,21,33,34] the I magnetization.

If the Hartmann–Hahn condition is satisfied, i.e.,

$$\gamma_I H_{1I} = \gamma_S H_{1S} , \tag{2}$$

then mutual I- and S-spin flips via the I–S dipolar interaction become energy conserving and cause the system to proceed rapidly to internal equilibrium. The result is a cooling of the S-spin system by the establishment of S-spin order (in the form of a magnetization along H_{1S}) and a small heating of the I-spin reservoir (a small decrease in the I magnetization). The effect on the I spins is very small since the S spins are rare. The process may be repeated by destroying the S-spin order and again bringing them into contact with the I spins. The destruction can be performed in several ways—in the Lurie–Slichter[35] experiment it is done by simply removing the H_{1S} field and allowing $\langle S\rangle$ to decay to zero.

If the cycle is repeated many times, the net effect is a substantial heating of the I-spin reservoir; subsequent observation of the I magnetization discloses a correspondingly large change leading to a greatly enhanced sensitivity in the detection of the S-spin resonance.

From the viewpoint of a spectroscopist, this experiment suffers from poor resolution. The I and S spins cannot be decoupled as described before since it is precisely their mutual interaction which constitutes the thermal link between their reservoirs and is necessary for the sensitive detection. We therefore make use of the I-spin reservoir only as a source of polarization, and instead of detecting the S spins indirectly via the I spins, we observe them directly. The experiment is then similar to the Lurie–Slichter version[35] (of the Hartmann–Hahn experiment)[31] described above, except that the S, and not the I magnetization is observed. Following the I–S contact (in the direct detection method we call this cross polarization), the S-spin decay is observed. Spin decoupling, and thus high resolution, is achieved by the same I-spin irradiation used for the spin locking. The cycle is repeated and the S signals accumulated until the I magnetization is depleted. This yields, of course, a large sensitivity enhancement over a conventional S free induction decay; we have therefore made some recognizable progress in our attack on the problem of sensitivity, making the present approach an attractive one for high-resolution NMR in solids.

The indirect detection methods can also be modified to yield improved resolution. Two approaches have been proposed and used in preliminary experiments. We shall see later that, depending on circumstances, these may or may not have advantages over our direct detection.

The next section describes our direct detection method, "proton-enhanced nuclear induction spectroscopy," in more detail, with reference to one typical version. Section III gives relevent experimental details and Sec. IV some exemplary results. In Sec. V we discuss briefly alternative versions of our experiment and finally, compare them with the indirect detection methods.

II. DESCRIPTION OF THE METHOD

In this section we present a more detailed account of our direct detection method. Since neither the spin-decoupling nor the double-resonance procedures are new, only the aspects relevant to the present experiments are discussed. Excellent quantitative details on the double-resonance phenomena can be found in several papers.[31,35,36] We indicate only how they are employed in a novel way for our purposes.

As mentioned in the Introduction, there are many variants to the experiment since the spin decoupling and cross polarization can be done in several ways. These will be discussed in Sec. V. For the present we have chosen to illustrate one simple version in order to make our presentation concrete. We shall see later that this may not be the best solution from the view of technical efficiency. Since the purpose of the experiment is to provide an enhanced sensitivity and resolution, we wish to compare it with conventional techniques; this is done next, following a brief theoretical digression.

A. Basic Theory

We consider the following system in a large external magnetic field: an abundant I spin system with a resonance frequency ω_{0I} is dipolar coupled to a rare S-spin system with resonance frequency ω_{0S}. Two strong rf fields with rotating components H_{1I} and H_{1S} are applied at frequencies ω_{0I} and ω_{0S}, respectively. This is illustrated in Fig. 2(a). The full Hamiltonian has the form,

$$\mathcal{H}=\mathcal{H}_0+\mathcal{H}_{dII}+\mathcal{H}_{dIS}+\mathcal{H}_{dSS}+\mathcal{H}_{1I}(t)+\mathcal{H}_{1S}(t)\,, \qquad (3)$$

where $\mathcal{H}_0$ is the Zeeman interaction of I and S spins with the external field, $\mathcal{H}_d$ is the full dipolar interaction, and $\mathcal{H}_{1I}(t)$ and $\mathcal{H}_{1S}(t)$ describe the coupling of the I and S spins to the rf excitation. As shown by Redfield,[32b] it is appropriate when $\mathcal{H}_{1I}$ and $\mathcal{H}_{iS}$ are strongly saturating to transform to a rotating frame in which the rf fields are stationary. In this case we need a double rotating frame induced by the transformation,[31]

$$R=\exp[-it(\omega_{0I}I_z+\omega_{0S}S_z)]\,. \qquad (4)$$

In this frame, the Hamiltonian is transformed to

$$\mathcal{H}_R=\mathcal{H}_d^0+\mathcal{H}_{1I}+\mathcal{H}_{1S}+\text{time-dependent terms}, \qquad (5)$$

where $\mathcal{H}_d^0$ has the form of Eq. (1), and

$$\mathcal{H}_{1I}=-\gamma_I\hbar H_{1I}\sum_i I_{ix}\,, \qquad (6)$$

$$\mathcal{H}_{1S}=-\gamma_S\hbar H_{1S}\sum_i S_{ix}\,. \qquad (7)$$

The phase of the rotation is chosen to put H_{1I} and

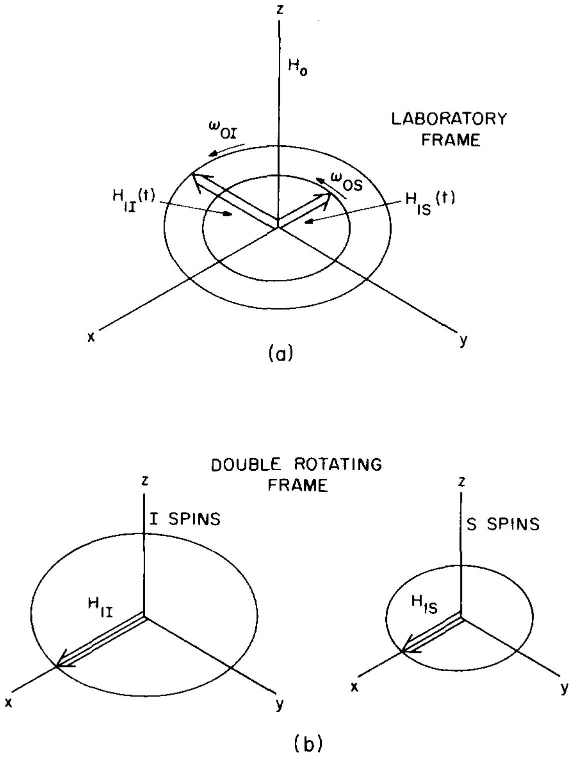

FIG. 2. Double-rotating frame transformation. In the laboratory frame (a) the rotating components of the I and S rf have amplitudes H_{1I}, H_{1S} and angular frequencies ω_I, ω_S. A rotating frame transformation, Eq. (4), is performed which rotates the I spins at ω_I and the S spins at ω_S about the Z axis. In this frame (b) we can imagine the I spins in their rotating frame experiencing a static field H_{1I} along x and the S spins in their rotating frame experiencing H_{1S} along x. The effects of H_{1S} on I spins and H_{1I} on S spins can be neglected if $\omega_I - \omega_S$ is much larger than the S and I spectral widths, as is normally the case.

H_{1S} along the x axes in the I and S rotating frames as in Fig. 2(b). Since we are not interested in calculating spin–lattice effects, we may discard the time-dependent terms, as is well known.

Thermodynamics can now be applied in the rotating frame since the Hamiltonian is effectively time independent.[32b] The two terms $\mathcal{H}_{1I}$ and $\mathcal{H}_{1S}$ are considered as reservoirs of Zeeman energy which exchange energy via the dipolar coupling with which they do not commute. The dipolar reservoir should also be included in the thermodynamics, but we shall neglect it for the present since we assume that H_{1I} is very large compared to internal local fields. Following Redfield, we assume that the system ultimately approaches a state of full internal equilibrium in the rotating frame described by the density matrix,

$$\rho_R^{\text{eq}} = \exp(-\beta\mathcal{H}_R)/\operatorname{Tr}\{\exp(-\beta\mathcal{H}_R)\}\,, \tag{8}$$

which for high temperatures and large fields is given to a good enough approximation for our purposes by

$$\rho_R^{\text{eq}} = Z^{-1}[1+\beta(\mathcal{H}_{1I}+\mathcal{H}_{1S})]\,, \tag{9}$$

where $Z = \operatorname{Tr}\{1\}$.

As pointed out by Hartmann and Hahn,[31] the rate at which this single spin temperature is approached depends strongly on the magnitudes of H_{1I} and H_{1S}. In general, each reservoir can be in internal equilibrium with a different spin temperature,[4]

$$\rho_R = Z^{-1}(1+\beta_I\mathcal{H}_{1I}+\beta_S\mathcal{H}_{1S}) \tag{10}$$

and the two subsystems come to equilibrium in a time T_{IS} (Fig. 1) which depends on $\gamma_I H_{1I} - \gamma_S H_{1S}$. When condition (2) is fulfilled, the rate is maximal as we shall see.

The quantities of interest to use are the energy, entropy, and magnetization. The Zeeman energy of the system in a state described by (10) is given by

$$E = -\operatorname{Tr}\{\rho_R\mathcal{H}_R\} = E_I + E_S = -\beta_I C_I H_{1I}^2 - \beta_S C_S H_{1S}^2\,, \tag{11}$$

where C_I and C_S are Curie constants given by

$$C_I = \tfrac{1}{3}\gamma_I^2\hbar^2 I(I+1)N_I \tag{12}$$

and similarly for C_S. N_I and N_S are the numbers of I and S spins.

The x component of the magnetization in the rotating frame (i.e., along the H_1 field) is given by

$$M_I = \gamma_I\hbar\langle I_x\rangle = \gamma_I\hbar\operatorname{Tr}\{\rho_R I_x\} = \beta_I C_I H_{1I} \tag{13}$$

and similarly for $\gamma_S\hbar\langle S_x\rangle = M_S$. Finally, the entropy is given by

$$S = -k\operatorname{Tr}\{\rho_R\log\rho_R\} = \text{const} - k\beta_I^2 C_I H_{1I}^2 - k\beta_S^2 C_S H_{1S}^2\,. \tag{14}$$

We now turn to an analysis of the experiments using these equations.

B. Free Induction Decay

Figure 3 shows how we would obtain a high resolution S spectrum by conventional techniques. The rare S system is allowed to equilibrate with the lattice in the external field H_0 for ~ T_{1S} at temperature β_L, yielding, from (13), a magnetization,

$$M_S^{(0)} = \beta_L C_S H_0\,. \tag{15}$$

This is observed in a free induction decay following a 90° pulse on the S spins.[37,38] The rf field on the I spins serves to decouple them, and Fourier transformation of the S decay yields a high resolution NMR spectrum. Before this can be repeated we must wait ~ T_{1S} again; in solids T_1's can be extremely long and thus sensitivity enhancement by signal averaging is rather painful. Since the S

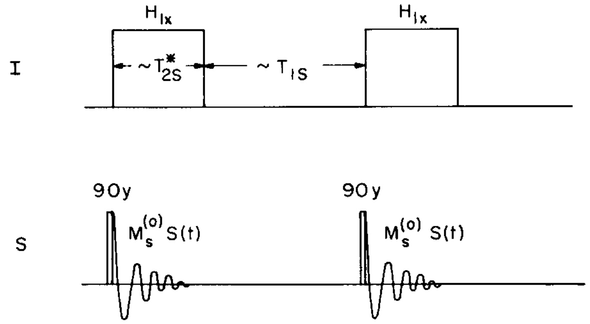

FIG. 3. Conventional high-resolution S free induction decay with I-spin decoupling. θ_y indicates a $\theta°$ pulse about the y axis of the appropriate rotating frame and H_{1x} continuous irradiation along x. The S spins are polarized every $\sim T_{1S}$ and then observed following a 90° pulse while continuously irradiating the I spins. For purposes of the analysis in the text it is imagined that $T_{1S} \gg T_{2S}{}^*$. $S(t)$ is the normalized S free induction decay.

spins are rare, the signals are small; for $S \equiv {}^{13}$C at low temperatures we might on occasion obtain tolerable signals, but if there are many lines, or if we are dealing with a less favorable isotope such as ^{15}N, then this approach becomes prohibitively difficult.

C. Cross Polarization

As we mentioned in the Introduction, the S-spin signal can be enhanced by using the abundant I-spin reservoir. The analysis follows exactly that due to Lurie and Slichter[35] except that we shall be inquiring into the accumulated S signal.

The experiment is illustrated in Fig. 4. In this case, the I spins are allowed to equilibrate with the lattice, yielding a magnetization,

$$M_I^{(0)} = \beta_L C_I H_0 . \tag{16}$$

This is now spin locked along the x axis in the I rotating frame, for example, by application of a 90_y pulse followed by a long phase-shifted pulse of amplitude H_{1I}.[33] Since the I and S systems are mutually isolated, we have

$$\rho_R^{(0)} = Z^{-1}(1 + \beta_0 \mathcal{H}_{1I}) \tag{17}$$

and from (13),

$$M_I^{(0)} = \beta_0 C_I H_{1I} \tag{18}$$

which is an operational definition of β_0, the I inverse Zeeman spin temperature in the rotating frame. From (16) and (17),

$$\beta_0 = \beta_L (H_0/H_{1I}) \tag{19}$$

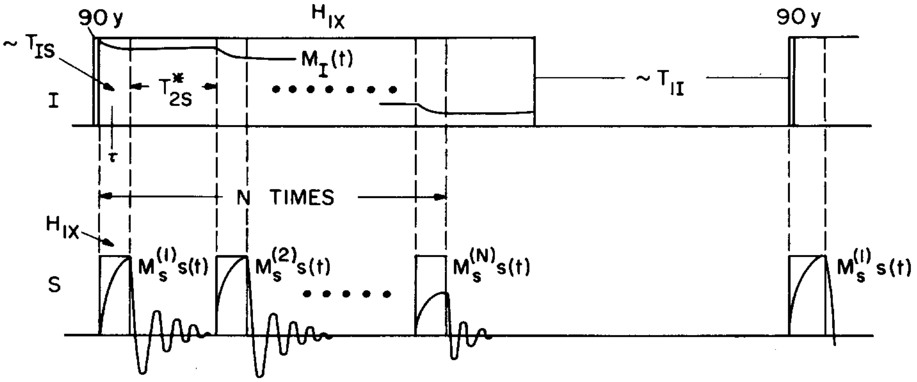

FIG. 4. One particularly simple version of proton-enhanced nuclear induction spectroscopy, using I–S cross polarization. After polarization of the I spins in $\sim T_{1I}$, the I magnetization is spin locked at resonance along H_{1I} in the I rotating frame (see Fig. 2). The S spins are brought into contact with the I reservoir by applying a resonant H_{1S} such that the Hartmann–Hahn condition, Eq. (2), is satisfied. The spin systems come rapidly to equilibrium causing a small decrease in M_I and a growth of M_S along their H_1 fields. This is indicated schematically in the figure by the curves inside the H_1 irradiation blocks. The H_{1S} field is then removed and the S free induction decay observed while continuing the I irradiation for spin decoupling. This is repeated N times and the S signals co-added until M_I is reduced to ~ 0. For the purposes of analysis in the text it is imagined that $T_{1\rho I}$, $T_{1I} \gg N(T_{2S}{}^* + T_{1S})$.

so this corresponds to a cooling of the I-spin system. The S spins (which are assumed unpolarized) are now coupled to the I by tuning on an rf field of amplitude H_{1S} along the x axis in the S rotating frame [see Fig. 2(b)]. The magnitude of H_{1S} is arranged to fulfill the Hartmann-Hahn condition (2) so that the I and S systems come rapidly ($\sim T_{IS}$) to equilibrium at a common spin temperature $\beta^{(1)}$, i.e.,

$$\rho_R^{(1)} = Z^{-1}[1+\beta_1(\mathcal{H}_{1I}+\mathcal{H}_{1S})]\,. \tag{20}$$

Since spin energy must be conserved in the equilibration process (spin-lattice relaxation times are long), we have, using (11), (17), and (20),

$$\beta_1 C_I H_{1I}^2 + \beta_1 C_S H_{1S}^2 = \beta_1 C_I H_{1I}^2\,. \tag{21}$$

Putting (2) into (21) and rearranging, we find

$$\beta_1 = \beta_0 (1+\epsilon)^{-1}\,, \tag{22}$$

where

$$\epsilon = \gamma_I^2 C_S / \gamma_S^2 C_I = S(S+1)N_S / I(I+1)N_I \tag{23}$$

and from (13), the S magnetization following this first thermal contact is

$$M_S^{(1)} = \beta_1 C_S H_{1S} = \beta_1 C_S (\gamma_I/\gamma_S) H_{1I}\,. \tag{24}$$

Using Eqs. (19) and (22) we find from (24),

$$M_S^{(1)} = (\gamma_I/\gamma_S)(1+\epsilon)^{-1}\beta_L C_S H_0$$

or since $\epsilon \ll 1$, to an excellent approximation,

$$M_S^{(1)} = (\gamma_I/\gamma_S)(1-\epsilon)\,\beta_L C_S H_0\,. \tag{25}$$

Recall from Sec. II B that if we had allowed the S spins to equilibrate directly with the lattice then from (15) we would have $M_S^{(0)} = \beta_L C_S H_0$; so looking at (25), we see that even in a single cross polarization we have gained a factor $(\gamma_I/\gamma_S)(1-\epsilon)$. This is ~4 for $I \equiv {}^1\mathrm{H}$, $S \equiv {}^{13}\mathrm{C}$ and ~10 for $I \equiv {}^1\mathrm{H}$, $S \equiv {}^{15}\mathrm{N}$.

The H_{1S} field is now removed and the decay of $M_S^{(1)}$ is observed. The S spins return to an unpolarized state. Then contact is established again, and going through the same procedure, we find after the nth such step,

$$M_S^{(n)} = (\gamma_I/\gamma_S)(1-\epsilon)^n M_S^{(0)}\,, \tag{26}$$

the signals resulting from these successive contacts are to be co-added and ultimately subjected to Fourier transformation to obtain the S-spin spectrum.

D. Sensitivity Considerations

For a further analysis of the efficiency of the cross-polarization experiment and comparison with alternative methods, it is useful to distinguish two limiting cases of experimental importance.

1. Case 1

The cross polarization is repeated until the I-spin magnetization has been largely or fully transferred to the S system, and the resulting signals co-added. Let the signal voltage at the beginning of the nonequilibrium S-spin free induction decay be $K_S M_S^{(0)}$ where K_S is an apparatus constant and $M_S^{(0)}$ is given in (15). The accumulated voltage after N cross polarizations is then, from (26)

$$V_S(N) = K_S(\gamma_I/\gamma_S) M_S^{(0)} \sum_{n=1}^{N} (1-\epsilon)^n$$

$$\approx K_S(\gamma_I/\gamma_S) M_S^{(0)} \sum_{n=1}^{N} e^{-n\epsilon}\,. \tag{27}$$

This signal is, of course, maximized by taking $N \to \infty$, but we must remember that successive signals decrease in amplitude in the presence of constant noise. If the rms noise voltage in the bandwidth of the detector is V_{nS}, the accumulated ratio of signal energy to noise energy is

$$\left(\frac{S}{N}\right)_{\mathrm{cp}} = \left(\frac{\gamma_I}{\gamma_S}\,\frac{K_S M_S^{(0)}}{V_{nS}}\right)^2 \frac{1}{N}\left(\sum_{n=1}^{N} e^{-n\epsilon}\right)^2. \tag{28}$$

This is maximized for

$$N\epsilon \equiv \lambda \sim 1.3\,, \tag{29}$$

for which

$$(S/N)_{\mathrm{cp}}^{(1)} = 0.41(\gamma_I/\gamma_S)^2 \epsilon^{-1} (K_S M_S^{(0)}/V_{nS})^2\,, \tag{30}$$

where the superscript (1) denotes the case under discussion.

The whole process can now be repeated, but to do so we must wait a time $\sim T_{1I}^{\dagger}$ for the I spins to become repolarized. (N. B.: In our experiments as performed to date, it is the ordinary T_1 which is appropriate. We allow for generality the possibility that a shorter effective time $T_{1I}^{\dagger}$ may become appropriate in other experiments where the reconvery to equilibrium occurs in the presence of an rf field near but not at ω_{0I}. The effective equilibrium magnetization $M_I^{(0)}$ would then also be altered causing an increase in the effective value of ϵ.) The efficiency of the cross-polarization experiment can then be discussed in terms of a figure of merit Q_{cp} which measures the over-all rate at which the signal energy climbs out of the noise. We have

$$Q_{\mathrm{cp}}^{(1)} = (T_{1I}^{\dagger})^{-1} (S/N)_{\mathrm{cp}}^{(1)}\,. \tag{31}$$

Remember that the above analysis is concerned only with the initial time point of the S-spin decay. The entire decay contains more information than that—a point to which we shall return in Sec. V. However, we are already in a position to make a direct comparison between the efficiencies of the cross-polarization experiment and the ordinary equilibrium free induction decay, since the time dependence of the recorded signals are identical. As above, we can write

$$(S/N)_{\mathrm{fid}} = (K_S M_S^{(0)}/V_{nS})^2\,. \tag{32}$$

Since this experiment requires a time $\sim T_{1S}$ rather than T_{1I} between replications, we define

$$Q_{\text{fid}} = (T_{1S})^{-1}(S/N)_{\text{fid}} . \qquad (33)$$

On the basis of the above we can define a gain in sensitivity resulting from use of the cross-polarization technique of

$$\mathcal{G}_{\text{cp}}^{(1)} \equiv Q_{\text{cp}}/Q_{\text{fid}} = (0.41/\epsilon)(\gamma_I/\gamma_S)^2(T_{1S}/T_{1I}^{\dagger}). \qquad (34)$$

For ^{13}C at natural isotopic abundance in organic solids, for which $N_I/N_S \sim 150$, we have $\mathcal{G}_{\text{cp}}^{(1)} \sim 10^3$ if $T_{1I}^{\dagger} = T_{1S}$. In fact usually $T_{1S} > T_{1I}$ and will become more so if paramagnetic doping is employed to speed relaxation, since there is more efficient diffusion of spin energy among the I spins. Thus the estimate of $\mathcal{G}_{\text{cp}}^{(1)}$ is perhaps pessimistic. Of course if the S spins are a still rarer species, and have a smaller value of γ_S, $\mathcal{G}_{\text{cp}}^{(1)}$ as calculated above will be much greater still—perhaps 10^5–10^6 in the case of ^{15}N in organic solids. As we shall see, however, such enormous gains for very rare spins are usually illusory in practice.

2. *Case 2*

The cross polarization is performed only once or a few times before the experiment is repeated. The usual reason for doing this is that the magnetization of the I system cannot be maintained for the desired time. Each cycle of cross polarization and signal recording requires a time of the order of $T_{IS} + T_{2S}^*$, where T_{2S}^* is the decay time corresponding to the obtainable frequency resolution δ_S: $\delta_S T_{2S}^* \approx 1$. T_{IS} is generally short and can be neglected in comparison to T_{2S}^*. In our experiments on ^{13}C, $T_{2S}^* \sim 0.01$ sec. Since the optimal number N of cross polarizations for this case is a few hundred, the exexperiment as analyzed under Case 1 would demand that H_{1I} be left on for periods of a few seconds. For rarer spins, e.g., ^{15}N, the corresponding time would be longer. This requirement may come into conflict with practical considerations concerning sample heating (*vide infra*), but often encounters a more fundamental obstacle embodied in the fact that the I magnetization decays with a characteristic rotating-frame spin-lattice relaxation time $T_{1\rho I} \leq T_{1I}^{\dagger}$ irrespective of the desired loss to the S system. When this effect is dominant, it becomes approximately appropriate to replace ϵ in (26)ff by $T_{2S}^*/T_{1\rho I}$. The final result is that (32) becomes

$$\mathcal{G}_{\text{cp}}^{(2)} = 0.41(\gamma_I/\gamma_S)^2(T_{1S}T_{1\rho I}/T_{2S}^*T_{1I}^{\dagger}), \qquad (35)$$

which is less favorable than before if $T_{1I}^{\dagger} = T_1$, as it was in our experiments. On the other hand it is sometimes the case that $T_{1I}^{\dagger}$ can be made appreciably shorter than T_1 by means of off-resonance irradiation. This is an important feature of an experiment of Bleich and Redfield to be discussed in Sec. V. In favorable cases, including especially many to which (35) is appropriate, one could have $T_{1I}^{\dagger} \sim T_{1\rho I}$ through appropriate off-resonance irradiation, and $\mathcal{G}_{\text{cp}}$ could again become quite large.

E. Adiabatic Transfer

Here we compare (34) with the most efficient process possible, namely an adiabatic one. We assume as in Fig. 5 that we can somehow transfer adiabatically (and thus reversibly) all the polarization from the I- to the S-spin reservoir. How this can be done does not concern us at present since we wish only to calculate a figure of merit for the above experiment. Suffice it to say that the process is indeed feasible[39] and will be discussed in detail elsewhere.

Before the transfer, all the polarization is in the I system and we assume the density matrix is given by (17). At the end of the transfer, the S spins only are polarized and thus

$$\rho_R^{\text{ad}} = Z^{-1}(1 + \beta_{\text{ad}}\mathcal{H}_{1S}). \qquad (36)$$

Since we postulate that the process is adiabatic we invoke conservation of entropy. Using Eq. (14) this tells us

$$\beta_0^2 C_I H_{1I}^2 = \beta_{\text{ad}}^2 C_S H_{1S}^2 . \qquad (37)$$

Inserting Eqs. (15), (16), and (23) into (37) and rearranging, we find for the final S magnetization

$$M_S^{\text{ad}} = (\gamma_I/\gamma_S)\sqrt{\epsilon}^{-1} M_S^{(0)} , \qquad (38)$$

which gives us for the data rate of our fixed point in exactly the same way as before

$$Q_{\text{ad}} = \mathcal{G}_{\text{ad}} Q_{\text{fid}} , \qquad (39)$$

where

$$\mathcal{G}_{\text{ad}} = \epsilon^{-1}(\gamma_I/\gamma_S)^2(T_{1S}/T_{1I}). \qquad (40)$$

Thus, looking at (35), we have lost only a factor of 0.41 in the cross-polarization technique. Con-

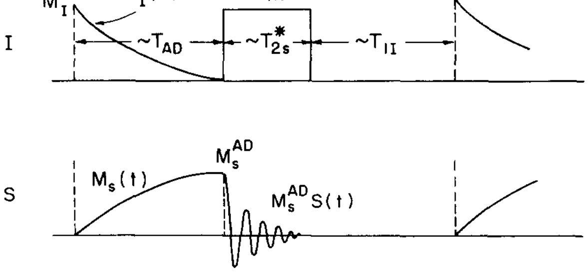

FIG. 5. Schematic representation of a complete adiabatic transfer of I-spin order into S-spin order and observation of the S signal. This is the most efficient process possible; magnetization can be calculated by imposing conservation of entropy. For the purposes of analysis it is assumed that $T_{1I} \gg T_{AD}$.

sidering the simplicity of our approach, this is certainly not a great price to pay.

A comparison of the sensitivity of these direct methods with various techniques of indirect detection will be made in Sec. V.

III. EXPERIMENTAL

The basic features of the pulsed NMR spectrometer used in these experiments have been described in detail elsewhere.[40-42] Changes were made to accommodate the double-resonance facilities, and these, together with the relevant experimental details, are described in this section. We also make some comparisons between spectrometer requirements for these experiments and those for multiple-pulse experiments.

A. Spectrometer

A schematic diagram of the spectrometer is shown in Fig. 6. The external magnetic field for our experiments was 2.28 T provided by an Oxford Instruments superconducting solenoid. The configuration shown is for ^{1}H (97.2 MHz) and ^{13}C (22.4 MHz). Two synthesizers provide the basic rf for the two frequencies. Operation is superheterodyne; the intermediate frequency of 30 MHz is split into four channels by a quadripole network.[43] Three of these, with relative phases of 0°, 90°, and 180°, are gated by the ^{1}H gating network, controlled by the pulse programmer, to produce the ^{1}H pulse sequence. Transmission of 97.2 MHz is from an amplified signal from the single (lower) sideband generator. This is necessary since the ^{1}H transmitter is a wideband device[44] and power must not be wasted in amplifying an unwanted sideband.

Since the final ^{13}C stage is tuned, SSB operation is not required for the 24.4 MHz and this is obtained directly from 54.4 MHz and the fourth 30 MHz channel. We will not go into a detailed discussion of power requirements, since these vary greatly from experiment to experiment. As an example, for the high Q 5 mm sample coils used in most of our ^{13}C work, ~200 W of rf power has been found to suffice for both final stages.

Reception of the 24.4 MHz signal is made with a tuned preamplifier (several have been used) and dual phase detection produces quadrature free induction decay signals for processing by complex Fourier transformation.[40,45] One problem in reception for these experiments is that of isolating the high-power ^{1}H frequency which leaks into the ^{13}C receiving system and produces large bias voltages at the preamplifier input. This problem is solved by use of crossed sample coils and by insertion of a multistage filter in the ^{13}C receiver line. With-

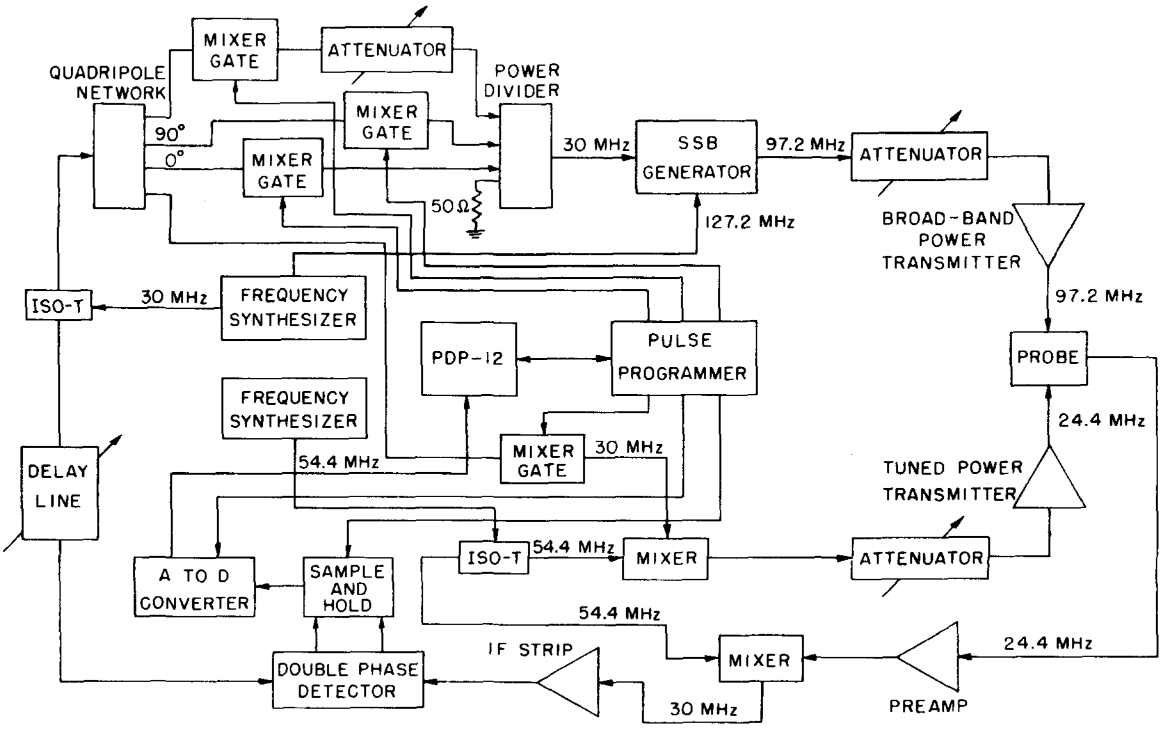

FIG. 6. Block diagram of double-resonance spectrometer shown in configuration for ^{13}C–^{1}H operation with ^{13}C detection.

out these precautions, detecting the small ^{13}C signals while irradiating the ^{1}H spins (decoupling) with high power rf is exceedingly difficult.

B. Probe

The low-temperature double-resonance probe, depicted in Fig. 7, is designed for operation in the superconducting solenoid geometry. A double coil is used; the inner one is a horizontal solenoid of diameter ~ 0.6 cm and length ~ 1.5 cm wound around the sample tube and used for the low-frequency transmission and reception. The outer is of bent Helmholtz ("saddle") geometry, insulated from the inner one by ~ 1 mm of Pyrex dielectric, and provides the high-power ^{1}H fields.

Matching and tuning of these coils is accomplished by standard techniques; the ^{13}C system can be tuned *in situ* by means of the variable capacitor which consists of two concentric copper tubes with a glass dielectric. The ^{1}H coil is connected via a half-wavelength coaxial cable with tuning and impedance matching performed remotely. The coaxial cables depicted contain high-temperature-resistant Teflon dielectric, since conventional materials are prone to melting on extended application of high-power rf.[46]

Temperature control is achieved in a standard way by passing dry nitrogen gas through a cooled copper coil and then into the sample chamber through evacuated transfer lines. Samples were prepared in cylindrical Pyrex ampuls with 0.5 cm o.d. and sealed under vacuum. It should be noted that this probe is a crude, preliminary one. The full exploitation of multiple-contact cross-polarization experiments, especially in the case of very rare spins would require a much more serious attack on the problem of heat dissipation.

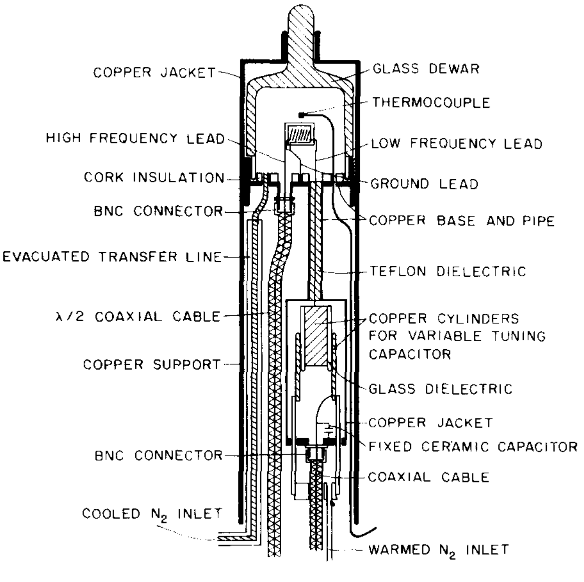

FIG. 7. Variable-temperature double-resonance probe adapted to geometry of superconducting solenoid.

C. Timing and Signal Processing

An important consideration for the initial period of experimentation for the double resonance was timing flexibility. Several versions of the experiment are possible and each had advantages and disadvantages which depend strongly on the circumstances. In the present spectrometer, timing is provided by a homebuilt pulse programmer[41] under control of an on line minicomputer (PDP-12). This provides variable pulsewidths and delays for the four rf channels and extremely flexible counting facilities. Pulse programs are entered through the computer from magnetic tape storage. This leads to very convenient interchangeability of programs and makes the experimentation with new versions and sequences a simple matter.

In addition to supervising the timing, the computer is also responsible for signal processing. After each cross polarization, the free induction decay is digitized and stored directly in computer core. Subsequent processing includes signal averaging, Fourier transformation, apodization and digital smoothing, plotting, mass storage, etc. The spectrometer operates with a dual phase detector, and advantage can be taken of this by using complex Fourier transformation which extends the effective spectral bandwidth by a factor of 2.

Timing requirements vary from experiment to experiment. Cross-polarization times vary in the range ~ 0.1–1 msec when condition (2) is satisfied. The decoupling time (~ T_{2S}^{*}) depends, of course, on the resolution achievable or desirable in the experiment. Ideally, this should approach the pure S–S dipolar broadening which for ^{13}C is expected to be of the order of ~ 10 Hz.[47] In practice, other limitations are inherent in our experiments, including magnetic field inhomogeneities and incomplete spin decoupling. Routinely we have operated with ~ 60 Hz linewidths (as evidenced from rigid single crystal studies) but have on occasion reduced linewidths to ~ 20 Hz in favorable cases. For ^{15}N, there is considerable broadening by the abundant ^{14}N isotope (~ 200 Hz) and data collection requires only ~ 10 msec per contact. Of course these requirements may change as auxiliary techniques such as sample spinning are implemented.

In favorable cases, where T_{1I} is not very long, a single cross polarization can be useful. One then obtains a single free induction decay per T_{1I} with γ_I/γ_S voltage enhancement. Many of our ^{13}C experiments were done in this way since the sensitivity is sufficient and sample heating by prolonged irradiation is avoided. For the less abundant isotopes, such as ^{15}N, multiple contacts were found to be essential.

D. Additional Comments

We make some final remarks concerning the stability requirements for these experiments as compared to the multiple-pulse techniques.[11-14] In multiple-pulse experiments, phase and amplitude stability are of crucial importance since the process requires long-term *coherent* excitation of the spins. Any instabilities will cause cumulative precessional phase lags between the spins and a subsequent rapid destruction of the magnetization. In addition, phase transients occur with the turn-on and turn-off of the rf pulses and these must either be minimized by using low Q probe circuits or a tedious amount of tuning must be performed to eliminate their effects. Since we are dealing, in the dilute spin case, with heteronuclear decoupling the requirements are considerably less stringent on several counts.

1. Power

Both experiments require sufficient rf field strengths to decouple spins interacting with strong dipolar couplings. However, in the double-resonance experiment, decoupling is continuous (since observation is at a different frequency); this means that multiple-pulse experiments require $1/\delta$ times the power to produce the same effective H_1 field (where δ is the duty factor), since power is proportional to H_1^2. An additional advantage of the continuous is indicated in consideration 3 below.

2. Stability

Neither the spin locking nor the spin decoupling require extraordinary stability of phase or amplitude of the rf. Only if quantitative cross-relaxation studies are the purpose of the research do stability requirements assume any importance, since T_{IS} is sensitive to the H_1's.

3. Probe Q

It is advantageous for the purposes of producing large H_1 fields and enhancing the sensitivity of signal detection to use high Q probe circuits. In multiple-pulse work this cannot be done indiscriminately since the magnetization must be sampled between closely spaced pulses, and receiver deadtime due to probe ringing becomes an important consideration. In the double-resonance experiments, of course, there is no such problem and high Q circuits like those used in liquid studies can be implemented. In fact our initial experiments have utilized circuits with $Q \sim 100$ at 24 MHz which is far greater than one is accustomed to in solid state multiple-pulse NMR.

Finally, we remark that the above considerations are not intended to imply that double-resonance always constitutes a wiser selection than multiple-pulse NMR, since they are appropriate to different conditions. For abundant spins such as ^{1}H, ^{19}F, the double-resonance procedure is irrelevant and one must resort to the more challenging technical requirements of multiple-pulse NMR. We believe that the two techniques will probably find their ultimate usefulness working in concert on the same systems—the multiple-pulse approach on the abundant spins (^{1}H, ^{19}F) and the cross polarization on the dilute spins (^{13}C, ^{15}N).

IV. RESULTS

In this section we present a discussion and some exemplary results to illustrate the utility and scope of the technique. Detailed and quantitative accounts of the experiments and results are given elsewhere and references will be made where appropriate.

A. Polycrystalline Samples

Our main interest in the preliminary experiments has been the measurement of chemical shielding anisotropies,[48] which are not available from the spectra of liquids. This information should be extremely valuable since it is related to molecular structure and is a much more severe test of chemical shielding theories than is the isotropic shift alone.

Remember that the chemical shift is a second-rank tensor (σ) which transforms under a rotation from (x, y, z) to (x', y', z') as

$$\sigma'_{ik} = \sum_{j,l} R_{ij} R_{kl} \sigma_{jl} \,. \tag{41}$$

In high field, only σ_{zz} in the laboratory system of coordinates is of interest[49]; if $R(\varphi, \theta, \psi)$ is the transformation from the principal axes (1, 2, 3) of σ to the laboratory system (x, y, z) in terms of the Euler angles φ, θ, ψ then the observed shift $\sigma \equiv \sigma_{zz}$ is given by

$$\sigma = \sin^2\theta \cos^2\varphi \sigma_{11} + \sin^2\theta \sin^2\varphi \sigma_{22} + \cos^2\theta \sigma_{33} \,, \tag{42}$$

where σ_{11}, σ_{22}, σ_{33} are eigenvalues of σ and we adopt the convention

$$\sigma_{11} \leq \sigma_{22} \leq \sigma_{33} \,. \tag{43}$$

In a polycrystalline sample, the effective chemical shift σ_{zz} must be weighted according to the isotropic probability distribution in (θ, φ), yielding the following absorption line shape derived by Bloembergen and Rowland,[50]

$$I(\sigma) \propto \begin{cases} [(\sigma_{33}-\sigma_{11})/(\sigma-\sigma_{11})]^{1/2} K(\sin\alpha) & \text{for } \sigma_{22}<\sigma<\sigma_{33} \\ [(\sigma_{33}-\sigma_{11})(\sigma_{33}-\sigma_{22})/(\sigma_{33}-\sigma)(\sigma_{22}-\sigma_{11})]^{1/2} & K[(\sin\alpha)^{-1}] \text{ for } \sigma_{11}<\sigma<\sigma_{22} \\ 0 & \text{elsewhere,} \end{cases} \tag{44}$$

where

$$\sin^2\alpha = (\sigma_{22}-\sigma_{11})(\sigma_{33}-\sigma)/(\sigma_{33}-\sigma_{22})(\sigma-\sigma_{11}) \tag{45}$$

and $K(k)$ is the complete elliptic integral of the first kind;

$$K(k) = \int_0^{\pi/2} (1-k^2\sin^2\gamma)^{-1/2}\, d\gamma . \tag{46}$$

This line shape is depicted in Fig. 8(a). σ_{11}, σ_{22}, and σ_{33} may be read off directly from the line shape. For a tensor with uniaxial symmetry, the line shape simplifies to

$$I(\sigma) \propto \begin{cases} (\sigma-\sigma_\perp)^{-1/2} & \text{for } \sigma_\perp<\sigma<\sigma_\parallel \\ 0 & \text{elsewhere ,} \end{cases} \tag{47}$$

where we have taken the case

$$\sigma_{11}=\sigma_{22}=\sigma_\perp , \quad \sigma_{33}=\sigma_\parallel . \tag{48}$$

This is shown in Fig. 8(b).

Although this is all well known, it is very seldom that such line shapes have been observed in NMR; except in unusual favorable cases[25,51–55] or where multiple-pulse techniques are applicable,[56] they are normally obscured by the strong dipolar broadening.

Figure 9 shows proton-enhanced ^{13}C spectra at natural isotopic abundance in some polycrystalline organic compounds at low temperatures. The low-field absorption is due to the carbonyl carbon in each compound. The line shapes conform to those in Fig. 8 and the elements of σ are read off with facility. Note the extreme sensitivity of σ_{22} to substituents. Methyl group ^{13}C shielding (e.g., the high-field absorption, Fig. 9) displays somewhat smaller anisotropies; an interesting feature in this case is that σ_{33} remains relatively unperturbed while σ_{11} and σ_{22} are very sensitive to the substituent.[57]

In this way we have determined the elements of σ for several low abundance nuclei including ^{13}C,[58–60] ^{29}Si,[61] and ^{15}N[62] in a variety of compounds in polycrystalline form.

Conditions for these experiments varied. Typically, for the ^{13}C and ^{29}Si work, high-frequency H_1 was ~12 G and low-frequency H_1 was ~40–50 G.

B. Single Crystal Studies

Although the principal values of σ are of great interest, valuable additional information could be obtained from the orientation of the principal axes in the molecular frame, thus specifying the full shielding tensor. In polycrystalline spectra this information is generally, but not always, lost. There are several ways to approach this problem, the most direct and clear-cut of which is by working with single crystals, where these are available. The paper immediately following this one gives a detailed account of such an investigation.

We mention briefly, in passing, that even when single crystals are not available, a substantial amount of orientational information may be extracted by auxiliary experiments. One possibility to be mentioned shortly depends on the existence of molecular motion. Another is to utilize dipolar splitting by a third nucleus (like or unlike S, unlike I). For ^{13}C–^{1}H, the third nucleus could be ^{13}C, ^{2}H, ^{14}N, etc. From the line shape in a polycrystalline sample, information can be obtained on the mutual orientation of the principal axes of σ and those of the dipolar interaction tensor. Since the latter

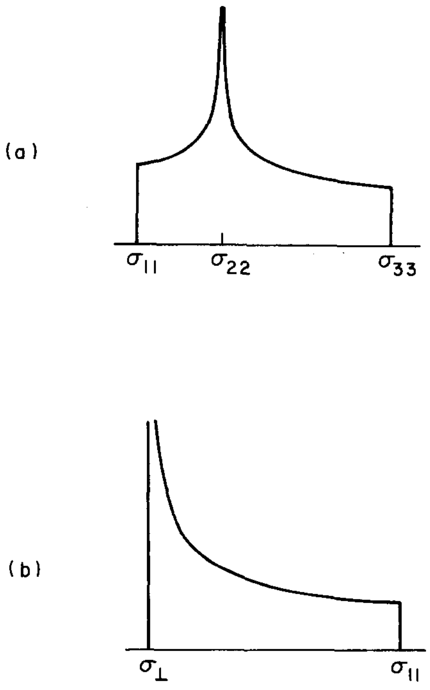

FIG. 8. Absorption line shapes for polycrystalline samples with (a) general, and (b) axially symmetric chemical shielding tensor σ. The line shapes are given by Eqs. (44) and (47). The principal values σ_{11}, σ_{22}, σ_{33} [$\sigma_{11}=\sigma_{22}=\sigma_\perp$, $\sigma_{33}=\sigma_\parallel$ in (b)] can be read off directly.

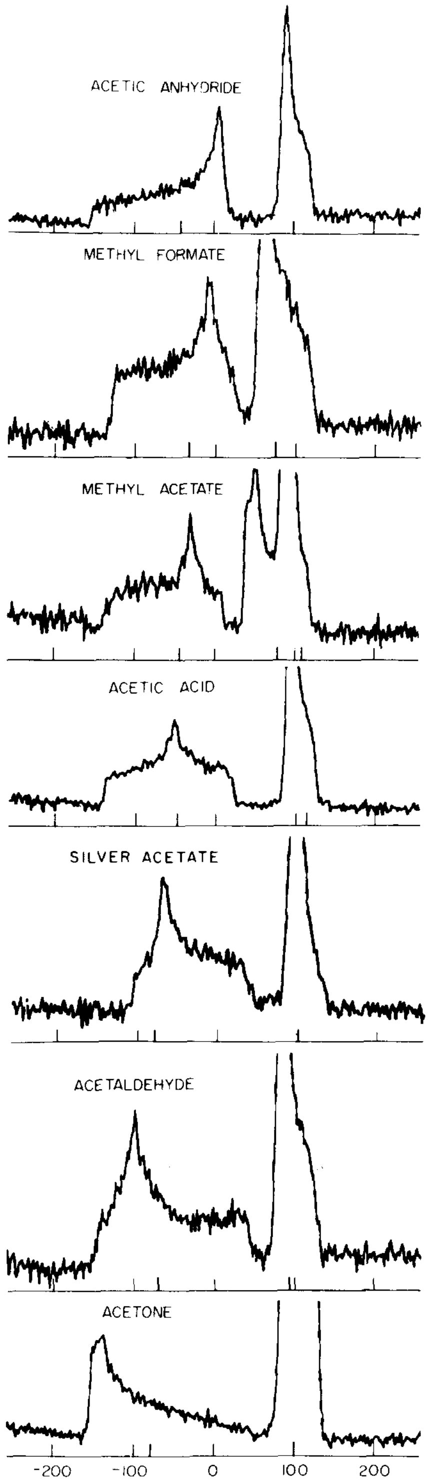

FIG. 9. Proton-enhanced ^{13}C spectra of polycrystalline compounds containing carbonyl groups. The low-field peaks are from the carbonyl and the high-field ones from methyl groups. The spectra were obtained using the sequence of Fig. 4 with various values of N, typically in a few minutes. Temperatures were all close to liquid nitrogen. Note the sensitivity of σ_{22} to substituents. The horizontal axis is calibrated in parts per million relative to an external reference of liquid benzene (23 °C).

have a well-defined orientation in the molecule this is a useful way of assigning σ to the molecular frame. An additional possibility is the study of cross-polarization times (see next section). A study of the differential cross-polarization times for different regions of the S spectrum should yield additional information on σ since these are also related to geometry through the orientation-dependent I–S dipolar interactions. Studies of both these types are in progress for several compounds from which crystals cannot be grown with facility.

C. Motional Effects

The type of spectra we have seen above may be severely modified in the presence of motion. Three types of motion are particularly relevant: (i) macroscopic sample rotation, (ii) molecular reorientation, (iii) molecular conformational changes.

In the case that (i) is performed about an axis inclined at the magic angle (54°44′) to H_0, it is easy to show that the average shift $\bar{\sigma} = \bar{\sigma}_{zz}$ over one cycle of rotation becomes independent of orientation and is given by the isotropic shift σ_i,[10]

$$\sigma_i = \mathrm{Tr}\,\sigma = \tfrac{1}{3}(\sigma_{11} + \sigma_{22} + \sigma_{33}) . \qquad (49)$$

This means that in a polycrystalline sample only a single sharp line will be observed for each inequivalent nucleus, at σ_i, if the above rotation is performed rapidly compared to the anisotropy spread $(\sigma_{33} - \sigma_{11})$. When this I–S dipolar interaction is considerably larger than $\sigma_{33} - \sigma_{11}$, this may provide a convenient means of retaining the sensitivity of the cross polarization and eliminating the broadening due to chemical shielding anisotropy where the latter is of no interest or difficult to evaluate due to overlapping peaks. It would certainly be a valuable accessory in the use of these techniques for structural studies in the solid state.[63]

The motion mentioned in (ii) may also manifest itself in these experiments and indeed may on occasion serve some useful purpose. A trivial case is that of rapid isotropic or nearly isotropic molecular reorientation in the solid. In this case the chemical shielding anisotropy is averaged to zero and we should expect to see a sharp line at σ_i. Since the intramolecular I–S dipole–dipole coupling is also averaged away, the proton-enhancement cross polarization proceeds entirely through the average intermolecular dipole–dipole coupling. A simple example of this phenomenon was provided by our early spectrum of adamantane using this technique.[23b] As is well known, adamantane undergoes rapid ($t_c \sim 10^{-11}$ sec) molecular rotation at 300 °K[64] and indeed two sharp lines were obtained in the solid ^{13}C spectrum.

An additional example is afforded by another "roundish" molecule, camphor, whose solid state ^{13}C spectrum exhibits eight resolved lines[59]; the spectrum compares well with the high resolution spectrum in solution.[65] Other molecules have been found to behave similarly including TMS, neopentane, cyclohexane, etc. In all these cases the requirements for proton H_1 fields are much less stringent in decoupling since the average dipolar interactions are reduced by the motion. Proton fields of ~3 G were found to produce acceptable decoupling.

A more interesting case is that of very anisotropic molecular motion, for example, restricted rotation about one axis in the molecule. When this is rapid, a partial averaging of the shielding tensor ensues.[56a] Again, the rotation may be described by the operator $R[\alpha, \beta, \gamma(t)]$ in terms of the Euler angles α, β, $\gamma(t)$ in the principal axes system; this is illustrated in Fig. 10. If an average is performed over $\gamma(t)$, we find for the effective shielding tensor σ the principal values,

$$\begin{aligned}&\bar{\sigma}_{33} = \bar{\sigma}_{\parallel} = \sin^2\beta\cos^2\alpha\sigma_{11} + \sin^2\beta\sin^2\alpha\sigma_{22} + \cos^2\beta\sigma_{33}\,,\\&\bar{\sigma}_{11} = \bar{\sigma}_{22} = \bar{\sigma}_{\perp} = \tfrac{1}{2}(3\sigma_i - \bar{\sigma}_{33})\,.\end{aligned} \tag{50}$$

So the average shielding tensor displays (as expected) axial symmetry about the rotation axis. This may be very helpful in polycrystalline samples for assigning $\sigma_{\parallel}$ to the molecular frame if something is known or assumed about the motion. On the other hand, where the orientation information is available from other sources (see the following), this may be used to learn a great deal about the nature of the motion.

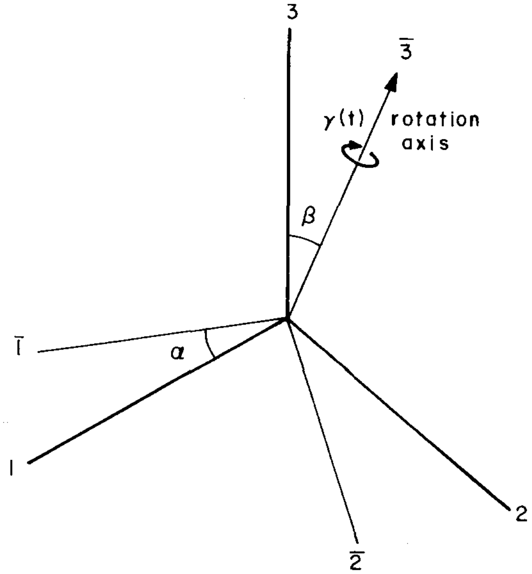

FIG. 10. Coordinate systems describing anisotropic molecular reorientation about one axis in the molecule. (1, 2, 3) are the principal axes of σ, ($\bar{1}$, $\bar{2}$, $\bar{3}$) are the rotating system about $\bar{3}$. When rotation is rapid, an average over $\gamma(t)$ is taken and one finds the average shielding tensor $\bar{\sigma}$ to be axially symmetric about $\bar{3}$. In the text it is shown how this may be used to lear about the orientation of (1, 2, 3) in the molecule.

We have reported a striking example of such behavior in polycrystalline hexamethylbenzene.[58] The low-temperature aromatic region of the ^{13}C spectrum exhibits an axial asymmetry and at high temperatures, with the onset of molecular motion the spectrum displays pseudoaxial symmetry with

$$\bar{\sigma}_{\parallel} = \sigma_{33}\,, \quad \bar{\sigma}_{\perp} = \tfrac{1}{2}(\sigma_{11} + \sigma_{22})\,. \tag{51}$$

This shows that $\beta = 0$ in (50), i.e., rotation is about the molecular axis 3 corresponding to σ_{33}. Since it is known that the motion in hexamethylbenzene,[66] like that in benzene,[67] consists of reorientation about the C_6 axis, this immediately assigns σ_{33}, the most shielded component, to the C_6 axis. The enhanced shielding of the ring carbons perpendicular to the aromatic plane has subsequently been verified in single crystal experiments.[68]

Finally, we mention that the motion indicated in (iii), molecular conformation change, may also be studied using these techniques. Solid state ^{13}C NMR should provide a powerful means of treating conformational processes in solids,[69] just as conventional NMR has served a vital role in studying these processes in liquids.[70] The information content in solid state spectral changes should be greater due to the orientational information contained in the chemical shielding anisotropy.

D. Cross-Polarization Dynamics

The theoretical discussion in Sec. II assumed that the cross-polarization step (Fig. 4) proceeded to full equilibrium between I and S. It is possible to learn alot about orientation and motion in solids by interrupting this step after a time τ and observing the high resolution S spectrum as a function of τ. This would measure the I–S cross-relaxation times for different lines or portions of the S spectrum in much the same spirit that high-resolution T_1 measurements are made in liquids.[71,72]

We forgo a detailed discussion of the cross relaxation since we have performed no quantitative experiments. We point out only the principal aspects of the theory relevant to our experiments and mention the possible potential in structural and dynamical studies.

If we assume that the coupling term $\mathcal{H}_{IS}^{0}$ in (5) is a perturbation on the large reservoir terms $\mathcal{H}_{1I}$ and $\mathcal{H}_{1S}$, then it is possible to arrive at an exponential form for the flow of energy between the I and S systems,[73]

$$(d/dt)(\beta_I - \beta_S) = -(T_{1S})^{-1}(\beta_I - \beta_S)\,. \tag{52}$$

The cross-relaxation time T_{IS} is calculated by the density matrix perturbation approach used by McArthur, Hahn, and Walstedt.[36] For the case of the resonant spin-locking version (Fig. 4) which we have discussed, one finds

$$1/T_{1S} = \tfrac{1}{2}\langle\Delta\omega^2\rangle_{IS} \int_0^\infty f(\tau)\cos\Delta\omega_1\tau\, d\tau\,, \tag{53}$$

where

$$\Delta\omega_1 = \gamma_1 H_{1I} - \gamma_S H_{1S}\,. \tag{54}$$

$\langle\Delta\omega\rangle_{IS}$ is the S second moment due to I–S dipolar interactions,

$$\langle\Delta\omega^2\rangle_{IS} = -\left[\mathrm{Tr}\left(\mathcal{H}^0_{IS}\sum_i S_{ix}\right)^2 \Big/ \mathrm{Tr}\left(\sum_i S_{ix}\right)^2\right]\,, \tag{55}$$

and $f(\tau)$ is the autocorrelation function of $\mathcal{H}^0_{IS}$ modulated by $\mathcal{H}^0_{II}$,

$$f(\tau) = \frac{\mathrm{Tr}(\sum_i b_i I_{ix})\exp[-(i/2\hbar)\mathcal{H}^0_{II}\tau](\sum_i b_i I_{ix})\exp[(i/2\hbar)\mathcal{H}^0_{II}\tau]}{\mathrm{Tr}(\sum_i b_i I_{ix})^2}\,. \tag{56}$$

$\mathcal{H}^0_{II}$, $\mathcal{H}^0_{IS}$, and b_i are given in Eq. (1). The form of $f(\tau)$ can be determined experimentally by measuring its Fourier transform $(T_{IS})^{-1}$ vs $\Delta\omega_1$ [since it is practically impossible to calculate $f(\tau)$ exactly] as in the work of McArthur, Hahn, and Walstedt.[36] We have not done this, but for the present assume that the behavior in our case is also exponential, i.e.,

$$(T_{IS})^{-1} \propto \exp(-\Delta\omega_1\tau)\,,$$

so (57)

$$f(\tau) = [1 + (\tau^2/\tau_c^2)]^{-1}\,.$$

The exact form of $f(\tau)$ is not crucial for the purposes of our discussion where the Hartmann–Hahn condition[31] (2) is satisfied, $\Delta\omega_1 = 0$. The correlation time τ_c is given, comparing (53) and (57) by

$$(\tau_c^2)^{-1} = -\tfrac{1}{8}\left\{\mathrm{Tr}\left[\mathcal{H}^0_{II}, \sum_i b_i I_{ix}\right]^2 \Big/ \mathrm{Tr}\left(\sum_i b_i I_{ix}\right)^2\right\}. \tag{58}$$

(We assume for simplicity $b_{im} = b_i$ independent of m.) Substituting this into (56) and taking the case that $\Delta\omega_1 = 0$, we get

$$(T_{IS})^{-1} = C_{IS}\langle\Delta\omega^2\rangle_{IS}\langle\Delta\omega^2\rangle_{II}^{-1/2}\,, \tag{59}$$

where $\langle\Delta\omega^2\rangle_{II}$ is the normal high-field truncated second moment,

$$\langle\Delta\omega^2\rangle_{II} = -\left\{\left[\mathrm{Tr}\left[\mathcal{H}^0_{II}, \sum_i I_{ix}\right]^2 \Big/ \mathrm{Tr}\left(\sum_i I_{ix}\right)^2\right]\right\}, \tag{60}$$

C_{IS} is given by

$$C_{IS} = 3\pi\left(\sum_{i\neq j} a_{ij}^2 \sum_i b_i^2 \Big/ \left\{N_I \sum_{i\neq j} a_{ij}^2[(2b_i + b_j)^2 + (b_i + 2b_j)^2]\right\}\right)^{1/2}\,, \tag{61}$$

and a_{ij} is the geometrical factor in (1) for I spins

$$a_{ij} = [-\gamma_I^2\hbar^2 P_2(\cos\theta_{ij})]/r_{ij}^3\,. \tag{62}$$

From (59) we see that the dependence of T_{IS} on geometry is contained predominantly in $\langle\Delta\omega^2\rangle_{IS}$ and to a lesser extent in the remaining factors. Typical values of $\langle\Delta\omega^2\rangle$ and C_{IS} indicate that T_{IS} should range ~ 0.1–1 msec for ^{13}C–^{1}H as we have indeed observed.

A good example of this behavior is exhibited by the ^{13}C NMR of solid polycrystalline benzene. Figure 11(b) shows the normal proton-enhanced spectrum with full cross polarization. The spectrum displays axial symmetry due to rapid reorientation about the C_6 axis, as discussed in Sec. IV A. The line shape is that of Eq. (47) [Fig. 8(b)] with σ given by

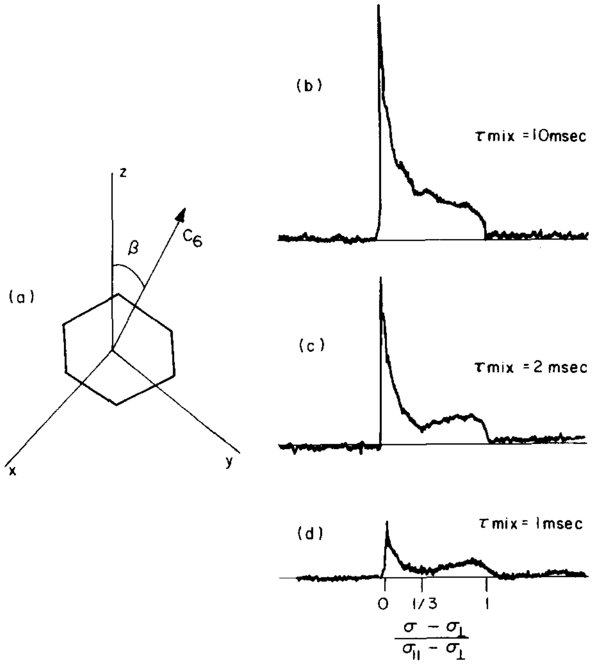

FIG. 11. Effects of incomplete cross relaxation in proton-enhanced ^{13}C NMR of solid polycrystalline benzene at −50 °C. The molecule is undergoing rapid reorientation about its C_6 axis which makes an angle β with H_0(a). The spectra are obtained from a single-contact version of Fig. 4 (N=1) with variable τ. For long $\tau > T_{IS}$ (b) we see a fully relaxed ^{13}C spectrum. For short τ, we see that ^{13}C in molecules with $P_2(\cos\beta) \sim 0$ [i.e., $(\sigma-\sigma_\perp)/(\sigma_\parallel-\sigma_\perp) \sim \frac{1}{3}$] cross polarize very slowly as expected from theory.

$$(\sigma-\sigma_\perp)/(\sigma_\parallel-\sigma_\perp)=\cos^2\beta\,, \tag{63}$$

where β is the angle between the C_6 axis and H_0 as shown in Fig. 12(a). Figures 12(c) and 12(d) show the effects of cross relaxation. For ^{13}C, the main contribution to $\langle\Delta\omega^2\rangle_{IS}$ is intramolecular and is given by

$$\langle\Delta\omega^2\rangle_{IS}=\langle\Delta\omega^2\rangle_0[P_2(\cos\beta)]^2\,, \tag{64}$$

where $\langle\Delta\omega^2\rangle_0$ is the intramolecular second moment for $\beta=0$, since the dipolar interaction is proportional to $P_2(\cos\beta)$. This predicts that the cross relaxation should be strongly inhibited at the magic angle (54° 44′) where $P_2(\cos\beta)=0$, i.e.,

$$(\sigma-\sigma_\perp)/(\sigma_\parallel-\sigma_\perp)=\tfrac{1}{3}\,. \tag{65}$$

This is indeed observed in Fig. 11 in agreement with the result obtained using indirect detection by Yannoni and Bleich.[74] Note, however, that the distortion due to cross relaxation is a necessary consequence of the latter technique, whereas it is an option in our direct detection method.

A quantitative study would necessitate a calculation of the intra- and intermolecular contributions to $\langle\Delta\omega^2\rangle_{IS}$, $\langle\Delta\omega^2\rangle_{II}$, and C_{IS} from the crystal structure. It is known, for example, that in benzene both contributions are about equal for $\langle\Delta\omega^2\rangle_{II}$.[67a] In addition, from the experimental point of view, a calibration of the H_1's would be essential—in our case this was not done due to a rather large instability in the amplitudes of the rf. Thus at present no quantitative discussion is pertinent and only the relative behavior discussed previously is meaningful. A full quantitative study of this system [including the case $\Delta\omega_1\neq 0$ to check the form of $f(\tau)$ in (56)] would be very interesting.

Another case which we have studied is solid adamantane at room temperature. There, both sharp ^{13}C lines are found to cross polarize at the same rate (~1 msec for the conditions of our experiment). This is in line with the isotropic motion notion which wipes out the anisotropy in $\langle\Delta\omega^2\rangle$. *Cross relaxation proceeds purely by intermolecular dipolar coupling.* If there were no motion, the carbon with two protons bonded would be expected to cross polarize more rapidly than that with one.

Preliminary results have also been reported for ^{13}C spin–lattice relaxation in solid benzene.[75] This is a useful additional experiment to the cross relaxation, and also fits in with the accepted model of anisotropic motion.[67] In adamantane, spin–lattice relaxation does distinguish the two carbons, that with two protons relaxing more rapidly (as expected for dipolar relaxation) as in solution.[76] Full details on these experiments will be presented separately.

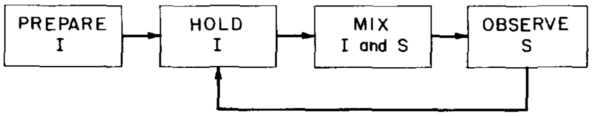

FIG. 12. Schematic general representation of direct detection double resonance such as proton-enhanced NMR. Examples of options for the various steps are presented in the text.

V. DISCUSSION OF VARIOUS METHODS FOR SPECTROSCOPY OF DILUTE SPINS

The discussion so far has centered on one particular version of the double-resonance experiment. This has served, we hope, to illustrate the main features of the technique. In this section we wish to point out that many versions are possible and that each one, or some combinations thereof, may be more advantageous in different circumstances. We first talk about alternative direct dedetection methods and then mention briefly some high-resolution modifications of indirect detection.

A. Direct Detection

For the purposes of this discussion it is convenient to reduce the direct detection methods to four major steps depicted schematically in Fig. 12. Step 1, preparation, is usually the polarization of I spins to full magnetization in H_0. The "hold" period is that during which the I-spin order must be maintained. In the version we have discussed, this is done in the I rotating frame by spin locking. "Mix" constitutes the transfer of spin order from the I to the S-spin system which was done by transfer of polarization from H_{1I} in the I rotating frame to H_{1S} in the S rotating frame. Finally, in the "observe" step the S signal is observed and recorded—the I spins may be decoupled if we desire high-resolution S spectra, or remain undecoupled if we are interested in broad-line S spectra. In our preceding version, decoupling was performed continuously by the I spin-locking field.

The following is not intended to be an encyclopedia of all the methods available as alternatives for the above steps. We wish only to point out illustrative examples. Many others will surely occur to the reader. Which one or which combination is best suited to the particular experiment at hand is largely a matter of the experimenter's discretion and may be the result, in some cases, of trial and error. We shall also indicate a few combinations suited for general application.

(1) Prepare
  (a) polarize I by spin–lattice relaxation in H_0,
  (b) dynamically polarize I by optical polarization,[77]
  (c) polarize I using polarized quadrupolar

nucleus with short spin–lattice relaxation time.[78]

(2) Hold
  (a) hold M_I along H_0 in laboratory frame,
  (b) spin lock M_I along H_{1I} in rotating frame,
  (c) hold I order in dipolar state in laboratory or rotating frame.[39]

(3) Mix
  (a) Hartmann–Hahn; matched or unmatched,
  (b) solid effect in laboratory or rotating frames,[79]
  (c) adiabatic crossover.[80]

(4) Observe
  (a) undecoupled I,
  (b) continuous I-spin decoupling,[28]
  (c) pulsed I-spin decoupling.[29]

The nature of these phenomena has been discussed in detail in the references cited. Matched and unmatched Hartmann–Hahn mixing refer to mixing satisfying, or not satisfying, Eq. (2), respectively. More generally, H_{1I} would be replaced by $\overline{H}_{1I}$ where $\overline{H}_{1I}$ is either some suitably defined average H_1 over a pulse train or a local dipolar field.[81,82]

An important consideration in these experiments is sample heating. In the version we talked about in Sec. II, long continuous irradiation of the I system is required and this may lead to unacceptable average power dissipation in the probe. This is the purpose of the hold period—to allow a cooling of the sample and probe while maintaining the I-spin order. A particularly useful option in this respect, just mentioned in 2(c), is the dipolar state, which we discuss now in a little more detail. This presents a means of storing I-spin order in the rotating frame without the need for strong spin-locking fields.

A low-temperature dipolar-ordered state may be obtained by transforming Zeeman order into dipolar order by one of several techniques, e.g.,[83]

(1) Adiabatic demagnetization in the rotating frame (ADRF)[84] following spin locking.

(2) ADRF by adiabatic fast passage with a small H_1 into resonance, and removal of H_1.

(3) $90_y - 45_x$ two-pulse transfer[85]—this is not adiabatic but is a simple and rapid way to make a ~50% efficient transfer.

Following such a conversion, the high-temperature density matrix may be treated as though it assumed the form,

$$\rho_{\mathrm{dip}} = Z^{-1}(1 + \beta_{\mathrm{dip}}\mathcal{H}_{II}^{0}), \tag{66}$$

with β_{dip} depending on the initial spin temperature and the technique used. The thermodynamical discussion in Sec. II is still valid if H_{1I} is replaced by H'_L, the local dipolar field defined by

$$\beta_{\mathrm{dip}} C_I H_L'^2 = \mathrm{Tr}\{\rho_{\mathrm{dip}}\mathcal{H}_{II}^{0}\} \tag{67}$$

to make the analogy with the Zeeman field H_{1I} in the expression for the Zeeman energy in (11). H'_L is given by

$$H_L'^2 = (3\gamma_I^2)^{-1}\langle\Delta\omega^2\rangle_{II}, \tag{68}$$

where $\langle\Delta\omega^2\rangle_{II}$ appears in (60). This is all well known and will not be enlarged on here. The main point is that this order may still be transferred from I to the S spins by application of an S field H_{1S} in the S rotating frame. The dynamics of this process have been treated in detail by McArthur, Hahn, and Walstedt[36] in the course of their study of ^{43}Ca–^{19}F double resonance.

Assume as in Sec. II C that we begin again with the I spins polarized at the lattice temperature and perform an ADRF. The density matrix is then given to a good approximation, in analogy to (17), by

$$\rho_R^{(0)} = Z^{-1}(1 + \beta_0\mathcal{H}_{II}^{0}), \tag{69}$$

where this time it is easily seen,

$$\beta_0 = \beta_L(H_0/H'_L). \tag{70}$$

We now turn on an S field H_{1S} at exact resonance such that

$$\gamma_S H_{1S} = \alpha\gamma_I H'_L. \tag{71}$$

The I and S spins now come to equilibrium with

$$\rho_R^{(1)} = Z^{-1}[1 + \beta_1(\mathcal{H}_{II}^{0} + \mathcal{H}_{1S})] \tag{72}$$

yielding, using exactly the same considerations as those leading to (22) and (25),

$$M_S^{(1)} = (\gamma_I/\gamma_S)[\alpha/(1+\alpha^2\epsilon)]M_S^{(0)} \tag{73}$$

with $M_S^{(0)}$ given by (15). The spin-locking case treated before corresponds to $H'_L \to H_{1I}$ and $\alpha = 1$ (Hartmann–Hahn condition). The cross-relaxation time T_{IS} for this type of experiment calculated by McArthur, Hahn, and Walstedt is[36]

$$1/T_{IS} = \langle\Delta\omega^2\rangle_{IS}\int_0^\infty a(\tau)\cos\alpha\omega'_L\tau\, d\tau, \tag{74}$$

where $\omega'_L = \gamma_I H'_L$ is constant and $a(\tau)$ is the same as $f(\tau)$ in (56) with I_{ix} replaced by I_{iz} and the $\frac{1}{2}$ removed from the exponents. Those authors measured an exponential dependence of T_{IS} on α, i.e., $(T_{IS})^{-1} \propto \exp(-\alpha\omega'_L\tau_c)$. If we assume this to be generally true then we can use Eq. (17) of their work,

$$(T_{IS})^{-1} = \tfrac{1}{2}\pi\langle\Delta\omega^2\rangle_{IS}\tau_c\exp(-\alpha\omega'_L\tau_c), \tag{75}$$

with τ_c given by (58) and I_{ix} replaced by I_{iz}.

Two interesting cases arise.

1. α ~ 1

In this case T_{IS} can still be short and one obtains after N cycles of transfer a magnetization $M_S^{(n)}$ given by (26) exactly as before. The signals from

$M_S^{(n)}$ are again co-added yielding about the same sensitivity as before. Several versions of this approach are illustrated in Fig. 13 which also shows some permissible combinations of decoupling sequences.

2. $\alpha \gg 1$

In this case we can obtain, looking at (73), a large S polarization in one shot. The maximal value of $M_S^{(1)}$ occurs for

$$\alpha\sqrt{\varepsilon} = 1\,, \tag{76}$$

where

$$M_S^{(1)} = (\gamma_I/\gamma_S)(2\sqrt{\varepsilon})^{-1}M_S^{(0)} \tag{77}$$

or one-half the polarization from an adiabatic transfer in (38). Adiabatic transfers are also possible as mentioned in Sec. IIE and will be discussed in detail elsewhere.

The preceding looks like a very profitable venture since we obtain a very large S polarization in one shot (if $\varepsilon \ll 1$). Note, however, from (75) that T_{IS} gets longer as α is increased and may become prohibitively long. This is especially bad since H_{1S} is then large and sample heating may become a problem. The form of $a(\tau)$ also becomes crucial: Gaussian behavior, which some authors have assumed, would make things even worse if $\omega_L' \tau_c/\sqrt{\varepsilon} \gg 1$ as would usually be the case for small ε. In any case, the final sensitivity or data rate is about the same as in the multiple contact version ($\alpha \sim 1$) if T_{1I} is long.

There is at least one case where (2) above may clearly offer a considerable advantage, namely in T_1 measurements of the S-spin system as discussed by McArthur, Hahn, and Walstedt.[36] In this case a single-shot large S polarization is very useful since there is no analogy to the co-addition of many S signals from a single I polarization if T_{1S} is long. It is thus worthwhile to put $\alpha \gg 1$ and accept the long T_{IS}. (The sample heating may be alleviated by periodically putting M_S along H_0.) Figure 14 shows an example of how we can adapt this approach to high-resolution T_1 studies in our direct detection scheme. This is similar to T_1 studies in liquids[71,72] except for the enhanced sensitivity.

Finally, note that the unmatched Hartmann-Hahn experiment ($\gamma_S H_{1S} = \alpha\gamma_I H_{1I}$) may be used to obtain large $M_S^{(1)}$ even in the spin-locking version of Sec.

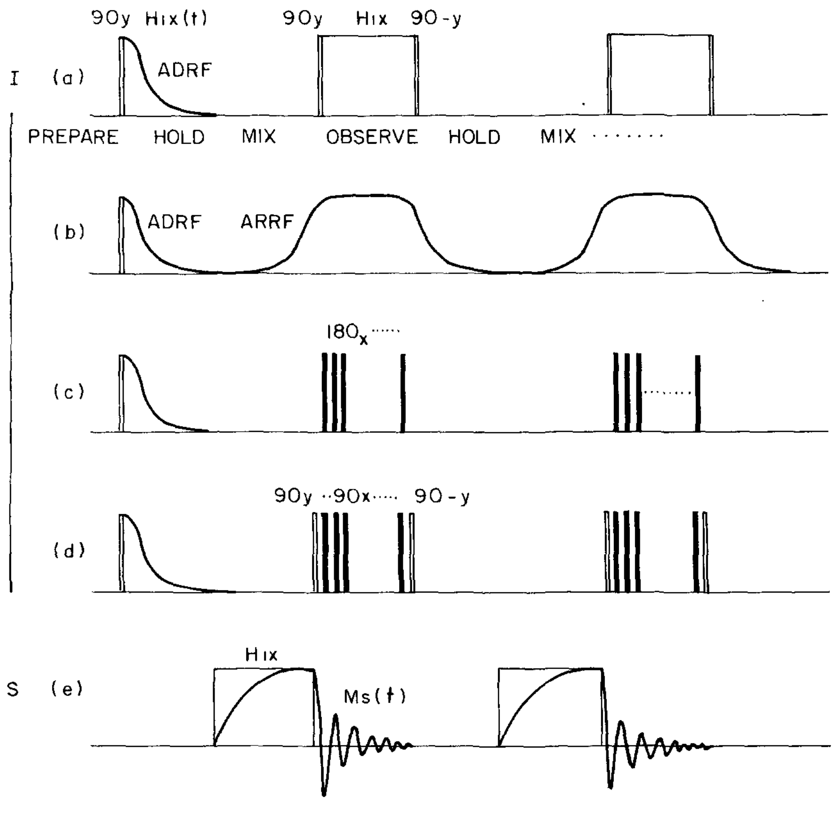

FIG. 13. Examples of high-resolution cross-polarization experiments using an I dipolar state in the rotating frame. The I dipolar state in each case is produced by an adiabatic demagnetization in the rotating frame (ADRF). The mixing in each case is between the I spins in the dipolar state and the S spins with field H_{1X}. The hold period is to allow the probe and sample to cool. Several mixing steps may be used for each holding one until heating is excessive. (a) The I spins are decoupled while in the dipolar state. The 90° pulses cause a "spin locking" of the I dipolar state (magic sandwich). Direct irradiation would cause a 75% destruction. (b) An adiabatic remagnetization in the rotating frame (ARRF) brings back the I magnetization along H_{1x} and it is spin locked and decoupled during S observation. (c) The I spins are maintained in the dipolar state and decoupled with 180° pulses. Since H_{II}^0 is invariant to a 180° rotation this does not affect the spin order. (d) Here the decoupling is done with 90° pulses (to which H_{II}^0 is not invariant), so the system must be spin locked by 90°_Y pulses. This is a pulsed version of (a). Many other versions are possible. (e) S-spin irradiation for mixing and observation.

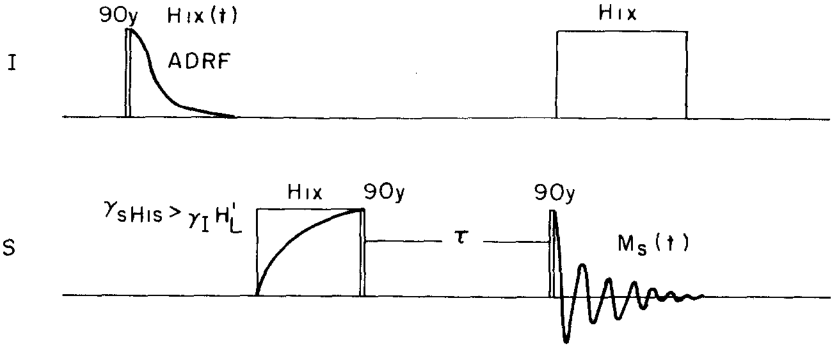

FIG. 14. Scheme for high-resolution study of S spin-lattice relaxation. The I spins are prepared in a dipolar state by ADRF. Cross polarization of the S spins is achieved with $\gamma_S H_{1S} > \gamma_I H_{1I}$ which gives a large S polarization (albeit more slowly, as explained in the text). This is placed along the Z axis and allowed to relax for a time τ. Subsequent observation with I-spin decoupling gives a high-resolution partially relaxed S spectrum. Again, many other versions are possible.

II. There, however, Eq. (62) for T_{IS} would read

$$(T_{IS})^{-1} = C_{IS}\langle\Delta\omega^2\rangle_{IS}\langle\Delta\omega^2\rangle_{II}^{-1/2}\exp[-(\alpha-1)\omega_{1I}\tau_c], \tag{78}$$

and we see that since ω_{1I} is large, this becomes much more sensitive to the unmatching.

B. Indirect Detection

Two modifications of the normal Hartmann–Hahn indirect detection method have been proposed for high resolution.[86,87] An obvious appeal of these techniques is that it is the abundant I spins which are observed making the signals much larger (due to number and usually higher Larmor frequency) than that of the direct S detection. This is not the whole story, however, since the indirect detection methods, signal strength notwithstanding, involve a mapping of the S spectrum point by point, and thus require long times to acquire the whole S spectrum. Thus, although the sensitivity may be very good, it may in some cases be *too* good, requiring long times, and making preferable the rapid S detection, *where the whole spectrum is obtained immediately*.

Figure 15 shows the high-resolution modification of the T_2 experiment of McArthur, Hahn, and Walstedt[36] used by Mansfield and Grannell.[87] The mixing and decoupling steps are performed through spin locking in the same way as for our direct detection scheme. Following the mixing step the S spins are allowed to undergo a decoupled (high-resolution) free induction decay for a time τ, and the mixing is performed again. If the normalized free induction decay is $S(t)$ as in IID and the above cycle is performed N times, then a cumulative destruction of the I magnetization ensues. Considerations similar to those used in Sec. II yield

$$M_I^{(N)} = M_I^{(0)}\exp\{-N\epsilon[1-S(\tau)]\}, \tag{79}$$

where $M_I^{(0)}$ is given by (16).

To prevent distortion of the signal it is necessary that

$$N\epsilon = \lambda \ll 1 \tag{80}$$

for which

$$M_I^{(0)} - M_I^{(N)} = \lambda M_I^{(0)}[1-S(\tau)] \tag{81}$$

so the destruction is proportional to $S(\tau)$. The S free induction decay can therefore be mapped out by plotting the destruction vs τ. For each point it is necessary to wait a time $\sim\lambda T_{1I}$ (or, if the experiment were suitably modified, $\lambda T_{1I}^{\dagger}$) for repolarization of the I system. If $\lambda \sim 1$ this can still be done, but a correction for distortion must be made.

Assume now that the voltage produced by $M_I^{(0)}$ is $K_I M_I^{(0)}$ and that, as in Sec. IID, the noise voltage in the detector bandwidth is V_{nI}. The data rate for

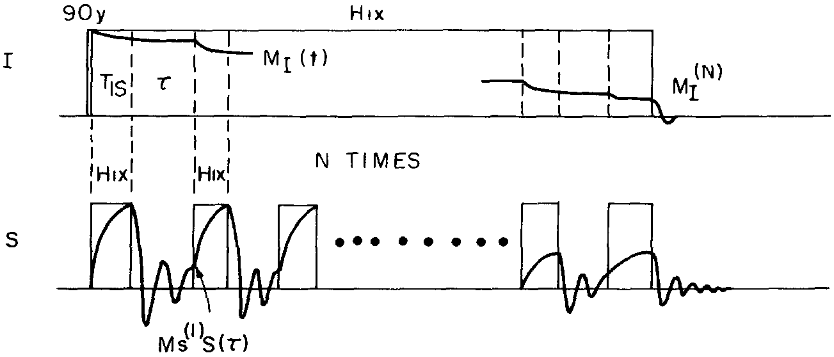

FIG. 15. Adaptation (Ref. 88) of indirect detection techniques to high resolution. In this case, the I spins are observed. Following an I–S contact (cross polarization) the S magnetization is allowed to decay, while decoupling I, for a time τ. This is performed N times with fixed τ_1 and the final I magnetization recorded. From the dependence of the I magnetization destruction on τ_1 the S free induction decay $S(\tau)$ may be extracted with very high sensitivity.

the signal point $S(\tau)$ is then

$$Q_{\mathrm{ind}}(\tau) \sim (\lambda/T_{1I}^{\dagger})[K_I M_I^{(0)} S(\tau)/V_{nI}]^2 . \tag{82}$$

We now note one important difference between the direct and indirect methods: In the former, the full decay $S(\tau)$ is obtained each time the I system is polarized. In the latter, each spin lock gives $S(\tau)$ only for one value of τ. Suppose that $S(\tau)$ contains Fourier components of frequencies up to Δ_S (the width of the S-spin spectrum in the frequency domain) and that $S(\tau)$ decays in a characteristic time T_{2S}^{*} (effective spectral resolution $\delta_S \sim 1/T_{2S}^{*}$). Then a total number $\Delta_S/\delta_S = \Delta_S T_{2S}^{*}$ of points must be collected before the experiment is replicated. Then the figure of merit to be compared with (34) or (35) is

$$Q_{\mathrm{ind}} = (\lambda/\Delta_S T_{2S}^{*} T_{1I}^{\dagger})(K_I M_I^{(0)}/V_{nI})^2 . \tag{83}$$

In writing (83) we have taken account of the fact that a measurement giving $S(\tau) = 0$ is as rich in information as one giving $|S(\tau)| = 1$: λ is to be chosen on the basis of the latter possibility.

To compare (83) with previous results, we again write

$$Q_{\mathrm{ind}} = \mathcal{G}_{\mathrm{ind}} Q_{\mathrm{fid}} \tag{84}$$

with

$$\mathcal{G}_{\mathrm{ind}} = (\lambda T_{1S}/\Delta_S T_{2S}^{*} T_{1I}^{\dagger})[K_I M_I^{(0)} V_{nS}/K_S M_S^{(0)} V_{nI}]^2 . \tag{85}$$

We then see, from (34) and (35), that approximately

$$\frac{Q_{\mathrm{cp}}^{(1)}}{Q_{\mathrm{ind}}} \approx (\Delta_S T_{2S}^{*}/\epsilon\lambda)(\gamma_I/\gamma_S)^2 [K_S M_S^{(0)} V_{nI}/K_I M_I^{(0)} V_{nS}]^2 \tag{86}$$

and

$$Q_{\mathrm{cp}}^{(2)}/Q_{\mathrm{ind}} \approx T_{1\rho I}\Delta_S(\gamma_I/\gamma_S)^2 [K_S M_S^{(0)} V_{nI}/K_I M_I^{(0)} V_{nS}]^2 . \tag{87}$$

In each case the factors preceding the ones in brackets favor the cross polarization and the factor in brackets favors the indirect method. Let us assume that $V_{nI} \approx V_{nS}$, which is tantamount to assuming that the requisite detector bandwidths T_{2I}^{-1} and Δ_S are comparable. The dependence of power signal-to-noise ratio on abundance and magnetogyric ratio, for a given field strength H_0, is such that

$$(K_S M_S^{(0)}/K_I M_I^{(0)})^2 \approx \epsilon^2 (\gamma_S/\gamma_I)^5 . \tag{88}$$

We assume that both detectors have the same noise figures and operate from the same coil Q. Then (86) and (87) become

$$Q_{\mathrm{cp}}^{(1)}/Q_{\mathrm{ind}} \approx (\epsilon\Delta_S T_{2S}^{*}/\lambda)(\gamma_S/\gamma_I)^2 \tag{89}$$

and

$$Q_{\mathrm{cp}}^{(2)}/Q_{\mathrm{ind}} \approx (\epsilon^2 T_{1\rho I}\Delta_S/\lambda)(\gamma_S/\gamma_I)^3 . \tag{90}$$

Representative values for $^{13}C-^{1}H$ spectroscopy are $\epsilon \approx 10^{-2}$, $\Delta_S \approx 10^4$ sec^{-1}, $T_{2S}^{*} \approx 10^{-2}$ sec. If we take $\lambda \approx 0.1$ as a reasonable compromise between sensitivity and lack of distortion, we see from (89) that the two methods have roughly the same sensitivity in Case 1, giving the cross-polarization method an advantage because of its relative simplicity and easy avoidance of distortions. When $T_{1\rho I}$ becomes relatively short, say, 0.1 sec, the indirect method begins to show an advantage according to (90). For species which are much more dilute or have a much smaller γ_S than ^{13}C, the advantages of indirect detection, particularly for short $T_{1\rho I}$, are felt in an important way.

Bleich and Redfield[86] have demonstrated a rather different indirect procedure. They switch rapidly but adiabatically between a "resonant" mode of duration t_R, during which the I magnetization varies as

$$dM_I/dt = \{[-\epsilon g(\omega)]/T_{IS}(\omega)\}M , \tag{91}$$

and a "monitor" mode of length t_M during which

$$dM_I/dt = (M_{eI} - M_I)/T_{1I}^{\dagger} . \tag{92}$$

Here M_{eI} is the semiequilibrium magnetization for off-resonance irradiation and $(T_{1I}^{\dagger})$, referred to several times earlier, is the rate constant for its achievement. $g(\omega)$ is the normalized S-spin absorption spectrum [Fourier transform of $S(t)$]. Account has been taken of the fact that T_{IS} is often different for different lines in the spectrum.

The experiment operates in a quasi-steady-state with $t_R \ll T_{IS}(\omega)$ and $t_M \ll T_{1I}^{\dagger}$. The solution of (91) and (92) under these conditions may be written in terms of the observed change in M_I as

$$M_{eI} - M(\omega) = M_{eI}\{\epsilon(\omega)/[\epsilon(\omega) + 1]\} , \tag{93}$$

where we define

$$\epsilon(\omega) = [\epsilon g(\omega) T_{1I}^{\dagger}/T_{IS}(\omega)](t_R/t_M) . \tag{94}$$

Note that the experimentally observed quantity $M_e - M(\omega)$ is a function not of the desired spectrum $g(\omega)$ but of $g(\omega)/T_{IS}(\omega)$. The resulting distortions are an inevitable consequence of the steady-state character of the method. This being the case, one might as well adjust experimental conditions so that that $M_{eI} - M_I(\omega) \approx M_{eI}$ for the strongest line in the spectrum. Then the power signal-to-noise ratio may approach

$$(S/N)_{\mathrm{ss}} \approx \mu (K_I M_I^{(0)}/V_{nI})^2 . \tag{95}$$

The dimensionless factor μ takes account of the facts that: (a) $M_{eI} < M_I^{(0)}$, (b) the signal is recorded only during t_M and not during t_R, and (c) even then the observation is done in time-shared fashion. A value of $\mu \approx 10^{-2}$ would probably be very optimistic, all things considered. In fact, for systems with rather short $T_{1\rho I}$ (to be compared with Case 2 of the cross-polarization method), competition between spin–lattice relaxation and cross relaxation will come to favor the former; we will then have $M_{eI} \ll M_I^{(0)}$ and $\mu \ll 1$.

To compare with other methods we must now take into account the following features of the steady-state (ss) experiment:

(a) Transient solutions of (91) and (92) show that the observed signal follows changes in $g(\omega)$ with a time constant ~ $T_{1I}^\dagger$. Accordingly the frequency sweep must be slow enough that a time at least $T_{1I}^\dagger$ is spent in scanning each resolution element (potential resolved line).

(b) There are $\Delta_S T_{2S}^*$ of these, so the replication time for each resolution element is $\Delta_S T_{2S}^* T_{1I}^\dagger$.

(c) Because of the slow scan, the detector noise bandwidth can advantageously be reduced to $\sim (T_{1I}^\dagger)^{-1}$, which is much narrower than the (roughly equal) values of Δ_S for the cross-polarization method or T_{2I}^{-1} for the Mansfield–Grannell experiment.

Taking all this into account, and incorporating (88) with proper attention to (c) above, we find

$$Q_{\mathrm{cp}}^{(1)}/Q_{\mathrm{ss}} \approx (\epsilon T_{2S}^*/\mu T_{1I}^\dagger)(\gamma_S/\gamma_I)^3 , \qquad (96)$$

$$Q_{\mathrm{cp}}^{(2)}/Q_{\mathrm{ss}} \approx (\epsilon^2 T_{1\rho I}/\mu T_{1I}^\dagger)(\gamma_S/\gamma_I)^3 . \qquad (97)$$

These look exactly like (89) and (90) except for the substitution of μ for λ and of $T_{1I}^\dagger$ for Δ_S^{-1}. The importance of the former is probably not great, and is so wrapped in the details of apparatus and its operation as to be beyond our powers to assess. The latter represents a considerable advantage, and arises from point (c) just mentioned. We have already remarked elsewhere[23] that the same advantage would be accessible to the Mansfield–Grannell procedure if it employed quasicontinuous observation during a time-shared spin lock.

What conclusions are to be drawn from this rough but protracted analysis? From the standpoint of sensitivity alone, the cross-polarization method works as well as anything else for spins which are moderately dilute, such as ^{13}C in natural abundance. For extremely dilute spins various indirect methods may become preferable. If spectral intensities are to be obtained without distortion, the cross-polarization method is called for when it can be used. This technique also seems to us to offer substantial advantages in experimental simplicity and ease of adjustment. Both the cross-polarization and Mansfield–Grannell methods require Fourier transformation, whereas the Bleich–Redfield experiment requires no computer.

We return now to a final point concerning sensitivity, but one that does not lend itself to a fully objective signal-to-noise analysis. Let us assume that $T_{1I}^\dagger \gg T_{2S}^*$, T_{IS}: This is essentially always true of solids and quasisolids. How much time is required to obtain the complete S-spin absorption spectrum, irrespective of sensitivity under optimum conditions? fid, $T_{1I}^\dagger$; cp, $T_{1I}^\dagger$; ind, $\Delta_S T_{2S}^* T_{1I}^\dagger$; ss, $\Delta_S T_{2S}^* T_{1I}^\dagger$. For typical spectra of chemical interest, $\Delta_S T_{2S}^* \sim 10^3$, i.e., both indirect methods take 100 times longer. Of the "quicker" methods, the cp method enjoys a substantial gain in sensitivity. Thus there exists a wide variety of circumstances under which the indirect methods, even when they enjoy an advantage in sensitivity, may make the experiment take more time than is tolerable considering the stability of the apparatus and of the experimenter and the subjective value of the information to be obtained.

The foregoing analyses of data rates, etc., have necessarily treated the time occupied in an experiment as having a fixed value, irrespective of how that time is spent. It is worth making the point that this is in practice not at all the case. Consider in connection with the cross-polarization experiment the following tactics: The time $T_{1I}^\dagger$ required to polarize the sample is spent with the sample (or preferably many samples) residing in a separate magnet of low homogeneity. When sufficient time has elapsed, the sample is adiabatically removed to the spectrometer magnet, and the spectrum recorded in the much shorter time NT_{2S}^* (*vide supra*). It is only this time which is expensive. That being so, it matters little how long $T_{1I}^\dagger$ is. We conceive of allowing it to be the rather long time T_{1I} necessary to polarize the sample at very low temperatures (4 °K or less) in a very strong magnetic field ($\sim 10^5$ G). There is then an enormous further gain ($\sim 10^5$) in power sensitivity resulting solely from the much increased thermal equilibrium polarization $M_I^{(0)}$, as compared with a situation in which the equilibrium polarization has been reached at room temperature in the weaker field of the spectrometer magnet. Rough absolute calculations show that the ^{13}C at natural abundance in a ~ 1 cm^3 sample of an organic solid should yield a total power signal/noise ratio in excess of 120 dB after a single such prepolarization. Thus we can envision the application of this technique to rather small samples containing very low concentrations of S spins.

ACKNOWLEDGMENTS

We are grateful to our colleagues W. K. Rhim, J. D. Ellett, Jr., R. G. Griffin, and S. Kaplan for continuing advice, assistance, and ideas. We especially thank M. Goldman, J. M. Deutch, A. G. Redfield, and C. S. Yannoni for a number of stimulating discussions concerning the theory of these experiments.

[*] Supported in part by the National Science Foundation and in part by the National Institutes of Health.

[†] Present address: Department of Chemistry, University of California and Inorganic Materials Research Division, Lawrence Berkeley Laboratory, Berkeley, CA 94720.

[‡] Present address: Center for Naval Analyses, 1401 Wilson Boulevard, Arlington, VA 22209.

[1] J. W. Emsley, J. Feeney, and L. H. Stucliffe, *High Resolution Nuclear Magnetic Resonance Spectroscopy* (Pergamon, London, 1967).

[2] (a) W. F. Wurzbach and S. Gade, Phys. Rev. B **6**, 1724 (1972); (b) E. T. Cheng and J. D. Memory, Phys. Rev. B **6**, 1714 (1972) and references cited therein; (c) D. K. Hutchins and S. M. Day, Phys. Rev. **180**, 432 (1969).

[3] Examples are: (a) I. J. Lowe and S. Gade, Phys. Rev. **156**, 817 (1967); (b) G. W. Leppelmeier and J. Jeener, Phys. Rev. **175**, 498 (1968); (c) W. E. Blumberg, Phys. Rev. **119**, 79 (1960); (d) D. Tse and S. R. Hartmann, Phys. Rev. Lett. **21**, 511 (1968); (e) N. Bloembergen, Physica (The Hague) **15**, 386 (1949).

[4] (a) J. Jeener, Adv. Magn. Reson. 3, 206 (1968); (b) A. G. Redfield, Science **164**, 1015 (1969); (c) M. Goldman, *Spin Temperature and Nuclear Magnetic Resonance in Solids* (Oxford U.P., London, 1970).

[5] (a) A. Abragam, *The Principles of Nuclear Magnetism* (Oxford U. P., London, 1961), Chaps. 4 and 7; (b) G. E. Pake, J. Chem. Phys. **16**, 317 (1948); (c) R. Bersohn and H. S. Gutowsky, J. Chem. Phys. **22**, 651 (1954).

[6] Examples are: (a) E. R. Andrew and R. Bersohn, J. Chem. Phys. **18**, 159 (1950); (b) H. S. Gutowsky and G. E. Pake, J. Chem. Phys. **18**, 162 (1950); (c) E. O. Stejskal and H. S. Gutowsky, J. Chem. Phys. **28**, 388 (1958); (d) T. B. Cobb and C. S. Johnson, Jr., J. Chem. Phys. **52**, 6224 (1970); (e) D. C. Look and I. J. Lowe, J. Chem. Phys. **44**, 2995 (1966); (f) D. W. McCall, Acc. Chem. Res. 33, 223 (1971).

[7] J. H. Van Vleck, Phys. Rev. **74**, 1168 (1948).

[8] (a) E. R. Andrew, A. Bradbury, and R. G. Eades, Arch. Sci. **11**, 223 (1958); (b) E. R. Andrew and V. T. Wynn, Proc. R. Soc. A **291**, 257 (1966).

[9] H. Kessemeier and R. E. Norberg, Phys. Rev. **155**, 321 (1967).

[10] E. R. Andrew, *Progress in NMR Spectroscopy* (Pergamon, New York, 1971), Vol. 8.

[11] J. S. Waugh, C. H. Wang, L. M. Huber, and R. L. Vold, J. Chem. Phys. **48**, 662 (1968).

[12] J. S. Waugh, L. M. Huber, and U. Haeberlen, Phys. Rev. Lett. **20**, 180 (1968).

[13] (a) U. Haeberlen and J. S. Waugh, Phys. Rev. **175**, 453 (1968); (b) U. Haeberlen and J. S. Waugh, Phys. Rev. **185**, 420 (1969).

[14] P. Mansfield, *Progress in NMR Spectroscopy* (Pergamon, New York, 1971), Vol. 8.

[15] P. Mansfield, J. Phys. C **4**, 1444 (1971).

[16] W.-K. Rhim, A. Pines, and J. S. Waugh, Phys. Rev. B **3**, 684 (1971).

[17] A. Pines, W.-K. Rhim, and J. S. Waugh, J. Magn. Reson. 6, 457 (1972).

[18] M. Mehring and J. S. Waugh, Phys. Rev. B **5**, 3459 (1972).

[19] C. H. Wang and J. D. Ramshaw, Phys. Rev. 6, 3253 (1972).

[20] U. Haeberlen, J. D. Ellett, Jr., and J. S. Waugh, J. Chem. Phys. **55**, 53 (1971).

[21] A. Pines and J. S. Waugh, J. Magn. Reson. 8, 354 (1972).

[22] R. W. Vaughan, D. D. Elleman, L. M. Stacey, W.-K Rhim, and J. W. Lee, Rev. Sci. Instrum. **43**, 1356 (1972).

[23] (a) A. Pines, M. G. Gibby, and J. S. Waugh, Bull. Am. Phys. Soc. **16**, 1403 (1971); (b) A. Pines, M. G. Gibby, and J. S. Waugh, J. Chem. Phys. **56**, 1776 (1972).

[24] P. C. Lauterbur, Phys. Rev. Lett. **1**, 343 (1958).

[25] A. Pines, W.-K. Rhim, and J. S. Waugh, J. Chem. Phys. **54**, 5439 (1971).

[26] T. C. Farrar and E. D. Becker, *Pulse and Fourier Transform NMR* (Academic, New York, 1971).

[27] J. M. Briggs, L. F. Farnell, and E. W. Randall, Chem. Commun. **1971**, 680

[28] L. R. Sarles and R. M. Cotts, Phys. Rev. **111**, 853 (1958).

[29] M. Mehring, A. Pines, W.-K. Rhim, and J. S. Waugh, J. Chem. Phys. **54**, 3239 (1971).

[30] A. Carrington and A. D. McLachlan, *Introduction to Magnetic Resonance* (Harper & Row, London, 1967), Chap. 13.

[31] S. R. Hartmann and E. L. Hahn, Phys. Rev. **128**, 2042 (1962).

[32] (a) A. Abragam and W. G. Proctor, Phys. Rev. **109**, 1441 (1958); (b) A. G. Redfield, Phys. Rev. **98**, 1787 (1955).

[33] I. Solomon, C.R. Acad. Sci. (Paris) **248**, 92 (1950).

[34] E. D. Ostroff and J. S. Waugh, Phys. Rev. Lett. **16**, 1097 (1966).

[35] F. M. Lurie and C. P. Slichter, Phys. Rev. **133**, A1108 (1964).

[36] D. A. McArthur, E. L. Hahn, and R. Walstedt, Phys. Rev. **188**, 609 (1969).

[37] I. J. Lowe and R. E. Norberg, Phys. Rev. **107**, 46 (1957).

[38] R. R. Ernst and W. A. Anderson, Rev. Sci. Instrum. **37**, 93 (1966).

[39] A. G. Anderson and S. R. Hartmann, Phys. Rev. **128**, 2023 (1962).

[40] J. D. Ellett, Jr., M. G. Gibby, U. Haeberlen, L. M. Huber, M. Mehring, A. Pines, and J. S. Waugh, Adv. Magn. Reson. 5, 117 (1971).

[41] A. Pines, Ph.D. thesis, MIT, 1972.

[42] M. G. Gibby, Ph.D. thesis, MIT 1972.

[43] Merrimac Research and Development, Inc., West Cadwell, NJ, custom built.

[44] Instruments for Industry, Inc., Famingdale, N.Y., Model M404P.

[45] A. G. Redfield and R. K. Gupta, Adv. Magn. Reson. 5, 81 (1971).

[46] A. Pines (unpublished results).

[47] C. Kittell and E. Abrahams, Phys. Rev. **90**, 238 (1953).

[48] (a) N. F. Ramsey, Phys. Rev. **78**, 699 (1951); (b) N. Bloembergen and T. J. Rowland, Phys. Rev. **97**, 1679 (1955); (c) P. Diehl and C. L. Khetrapal, *NMR: Basic Principles and Progress* (Springer, Berlin, 1969), Vol. 1; (d) A. D. Buckingham and K. A. McLauchlan, *Progress in NMR Spectroscopy* (Pergamon, New York, 1967), Vol. 2; (e) Reference 5(a), Chap. 6.

[49] The terms containing other elements are nonsecular in high field (oscillate rapidly) and cause only small second-order shifts.

[50] N. Bloembergen and T. J. Rowland, Acta Metall. **1**, 731 (1953).

[51] J. L. Ragle, J. Chem. Phys. **35**, 753 (1961).

[52] D. L. VanderHart, H. S. Gutowsky, and T. C. Farrar, J. Chem. Phys. **50**, 1058 (1969).

[53] N. Bloembergen and T. J. Rowland, Phys. Rev. **97**, 1679 (1955).

[54] D. K. Hindermann and W. E. Falconer, J. Chem. Phys. **52**, 6198 (1970).

[55] M. G. Gibby, A. Pines, W.-K Rhim, and J. S. Waugh, J. Chem. Phys. **56**, 991 (1972).

[56] M. Mehring, R. G. Griffin, and J. S. Waugh, J. Chem. Phys. **55**, 746 (1971).

[57] This is in line with recent theoretical calculations on ^{13}C shielding using gauge invariant orbitals: R. Ditchfield (private communication).

[58] A. Pines, M. G. Gibby, and J. S. Waugh, Chem. Phys. Lett. **15**, 373 (1972).

[59] J. S. Waugh, M. G. Gibby, S. Kaplan, and A. Pines, Colloque AMPERE, Turku, Finland, 1972 (to be published).

References 58 and 59 report measurements on a large number of organic compounds.

[60] A. Pines, R. G. Griffin, S. Kaplan, and J. S. Waugh (to be published).

[61] M. G. Gibby, A. Pines, and J. S. Waugh, J. Am. Chem. Soc. **94**, 6231 (1972).

[62] M. G. Gibby, A. Pines, R. G. Griffin, and J. S. Waugh, Chem. Phys. Lett. **17**, 80 (1972).

[63] (a) J. Schaeffer, presented at the 13th Experimental NMR Conference Asilomar, CA, 1972; (b) J. Schaeffer, S. H. Chin, and S. I. Weissman (to be published).

[64] H. A. Reising, Mol. Cryst. Liq. Cryst. **9**, 101 (1969).

[65] P. V. Demarco, D. Doddrell, and E. Wenkert, Chem. Commun. **1969**, 1418.

[66] (a) P. S. Allen and A. Cowking, J. Chem. Phys. **47**, 4286 (1967); (b) J. E. Anderson and W. P. Slichter, J. Chem. Phys. **44**, 1797 (1966); (c) H. W. Bernard, J. E. Tanner, and J. G. Aston, J. Chem. Phys. **50**, 5016 (1969).

[67] (a) E. R. Andrew and R. G. Eades, Proc. R. Soc. A **218**, 537 (1953); (b) J. E. Anderson, J. Chem. Phys. **43**, 3575 (1965); (c) R. van Steenwinkel, Z. Naturforsch. A **24**, 1526 (1969); (d) U. Haeberlen and G. Maier, Z. Naturforsch. A **22**, 1236 (1967); (e) U. Haeberlen, Z. Naturforsch. A **25**, 1459 (1970).

[68] S. Pausak, A. Pines, and J. S. Waugh, J. Chem. Phys. 58, 591 (1973).

[69] J. D. Ellett, Jr., U. Haeberlen, and J. S. Waugh, J. Am. Chem. Soc. **92**, 411 (1970).

[70] C. S. Johnson, Jr., Adv. Magn. Reson. 1, 223 (1965).

[71] R. L. Vold, J. S. Waugh, M. P. Klein, and D. E. Phelps, J. Chem. Phys. **48**, 3831 (1968).

[72] A. Allerhand, D. Doddrell, and R. Komoroski, J. Chem. Phys. **55**, 189 (1971).

[73] R. T. Schumacher, Phys. Rev. **112**, 837 (1958).

[74] C. S. Yannoni and H. E. Bleich, J. Chem. Phys. **55**, 5406 (1971).

[75] M. G. Gibby, A. Pines, and J. S. Waugh, Chem. Phys. Lett. **16**, 256 (1972).

[76] K. F. Kuhlman, D. M. Grant, and R. K. Harris, J. Chem. Phys. **52**, 3439 (1970).

[77] J. P. Colpa, K. H. Hausser, and D. Stehlik, Z. Naturforsch. A **26**, 1792 (1971).

[78] M. Goldman and A. Landesman, Phys. Rev. **132**, 610 (1963); M. Schwab and E. L. Hahn, J. Chem. Phys. **52**, 3152 (1970); Y. Hsieh, J. C. Koo, and E. L. Hahn, Chem. Phys. Lett. **13**, 563 (1972).

[79] Reference 4(c), Chap. 7.

[80] Reference 4(c), Chap. 6.

[81] P. Mansfield, K. H. B. Richards, and D. Ware, Phys. Rev. B 1, 2048 (1970).

[82] (a) E. P. Jones and S. R. Hartmann, Phys. Rev. Lett. **22**, 867 (1969); (b) E. P. Jones and S. R. Hartmann, Phys. Rev. B **6**, 757 (1972).

[83] An excellent discussion with leading references is given in Ref. 4(c), Chaps. 2 and 3.

[84] C. P. Slichter and W. C. Holton, Phys. Rev. **122**, 1701 (1961).

[85] J. Jeener and P. Broekaert, Phys. Rev. **157**, 232 (1967).

[86] H. E. Bleich and A. G. Redfield, J. Chem. Phys. **55**, 5405 (1971).

[87] P. Mansfield and P. K. Grannell, J. Phys. C **4**, L197 (1971).

[88] I. Solomon and J. Ezratty, Phys. Rev. 127, 78 (1962).